STATISTICS, OPTIMIZATION AND INFORMATION COMPUTING
Stat., Optim. Inf. Comput., Vol. **x**, Month 202x, pp 0–33.
Published online in International Academic Press (www.IAPress.org)

Classical and Bayesian Inference for the Transmuted Perk Distribution: Applications in Cancer Research and Engineering Reliability

Mohammed Elgarhy [1,2], Doaa Basalamah [3,*], Ahmed Mohamed El Gazar [4], Dina A. Ramadan [5], Ghareeb A. Marei [1], Neema M. Elharoun [6]

[1] *Faculty of Computers and Information Systems, Egyptian Chinese University, Nasr City, Egypt*
[2] *Department of Computer Engineering, Biruni University, 34010, Istanbul, Turkey*
[3] *Mathematics Department, Faculty of Sciences, Umm Al-Qura University, Makkah, Saudi Arabia*
[4] *Department of Basic Sciences, Higher Institute for Commercial Sciences, Almahlla Alkubra, Egypt*
[5] *Department of Mathematics, Faculty of Science, Mansoura University, Mansoura 33516, Egypt*
[6] *Department of Statistics and Insurance, Faculty of Commerce, Arish University, El-Arish 45511, Egypt*

Abstract Industrial and medical data are generally complicated and display variability, skewness and heavy tails, which makes accurate analysis a challenging task. These complexities are sometimes poorly represented by conventional probability distributions leading to incorrect results. In this paper, we propose the transmuted Perk (TP) distribution, as a new extension of the Perk (PE) distribution, by using a transmuted transformation technique to overcome the current problems. The density plot of the transmuted Perk distribution suggests its potential for practical applications. The hazard rate function (HRF) may exhibit increasing, decreasing and unimodal patterns, therefore offering great flexibility in the formulation of statistical models. Also computed are some reliability metrics, moments, inverse moments, moment generating function, quantile function and order statistics. Five classical methods were considered for the estimation of the parameters of the TP distribution, namely the maximum product of spacings (MPS), as referred (M_1), least squares (LS), as referred (M_2), weighted least squares (WLS), as referred (M_3), Cramer Von-Mises (CM), as referred (M_4) and Anderson-Darling (AD), as referred (M_5). In addition, a simulation exercise was conducted to assess the performance of these parameters. Furthermore, a comparative inference between the maximum likelihood estimation (MLE) and Bayesian methods was performed to derive the estimators of the parameters for the TP model. The proposed distribution was implemented on two real datasets from biological and industrial domains to show its practical usefulness. The goodness-of-fit was investigated using different measures and the results show that the TP model provides a much better fit than some of the classic distributions. The TP distribution is suggested for data analysis in engineering and biomedical disciplines since it fits better than the existing models.

Keywords Perk distribution, transmuted generated family, inverse moments, quantile function, least square estimation, real datasets

AMS 2010 subject classifications 62E10, 62F10, 62F15, 62N05

DOI: 10.19139/soic-2310-5070-5035

1. Introduction

Standard lifetime distributions are often not flexible enough for the complex shapes of real time-to-failure data, and a poorly specified model can lead to misleading conclusions about the reliability of a system or the survival of patients. The normal distribution is intrinsically unsuitable for asymmetric data, and the exponential distribution is inflexible because its hazard rate is constant and its density shape is fixed. The three-parameter Weibull distribution

*Correspondence to: Doaa Basalamah (Email: dabasalamah@uqu.edu.sa). Mathematics Department, Faculty of Sciences, Umm Al-Qura University, Makkah, Saudi Arabia.

ISSN 2310-5070 (online) ISSN 2311-004X (print)
Copyright © 202x International Academic Press

may not suit some failure-time analyses because its location parameter introduces a time shift that can distort an assessment of reliability or survival, while a two-parameter Weibull model with a zero-location assumption can lead to highly misleading conclusions [1]. Instead of changing the data to fit the model assumptions, a more effective approach is to extend existing models with additional shape parameters. Important examples are the generalized inverted Kumaraswamy-G [4], type II half-logistic odd Fréchet-G [5], Marshall–Olkin odd Burr III-G [6], transmuted exponentiated generalized-G [7], type I half-logistic Burr X-G [8], Teissier-G [9], odd inverse Weibull-G [10] and shifted Lomax-G [11] families. Several new lifetime models have also been introduced recently for engineering and biomedical data, such as the Marei [56], extended Lindley [50], odds-based Weibull [45] and one-parameter decreasing-hazard [57] models. For more details see [51, 52, 53, 54, 55, 2].

A simple way of adding a parameter to an existing distribution was introduced by Shaw and Buckley [12] through the quadratic rank transmutation map (QRTM). The resulting transmuted generated (T-G) family contains the parent distribution as a special case and has the cumulative distribution function (CDF) and probability density function (PDF)

$$F(w) = G(w)\left[1 + \lambda - \lambda G(w)\right], \qquad w \in \mathbb{R}, \quad |\lambda| \leq 1, \tag{1}$$

and

$$f(w) = g(w)\left[1 + \lambda - 2\lambda G(w)\right], \qquad w \in \mathbb{R}, \quad |\lambda| \leq 1, \tag{2}$$

where $G(w)$ is the CDF of the baseline model, $g(w)$ and $f(w)$ are the PDFs associated with $G(w)$ and $F(w)$, and λ is the transmuted parameter; the baseline is recovered at $\lambda = 0$. The T-G density is a mixture of the baseline density and the density of the minimum ($\lambda > 0$) or the maximum ($\lambda < 0$) of two independent baseline lifetimes, so $\lambda > 0$ shifts weight toward earlier failures and $\lambda < 0$ toward later ones. Many distributions have been built in this way, including the transmuted exponential power [13], Ishita [14], Mukherjee–Islam [15], Janardan [16], power Chris-Jerry [17], exponential-compound Weibull [18] and power unit inverse Lindley [19] models; see also [20] and [21], and inverse unit Teissier [40]. Recently, papers discussed some reliability measures such as, [41, 42, 43], including stress-strength reliability under progressive censoring, record data and unified hybrid censoring [44, 47, 49, 58], and inference for step-stress and progressively censored lifetime models [46, 48].

The Perk (PE) distribution [22] is a well-known lifetime model used in actuarial science, especially for the mortality of the elderly (Richards [23]). Several extensions of it have been proposed: the exponentiated Perk model of Singh and Choudhary [24], the Odd Perk-G family of [25], which has two scale parameters, and the inverse power Perk model of [26]. With parameters $\alpha > 0$ and $\theta > 0$, the PDF and CDF of the Perk distribution are

$$g(w) = \frac{\alpha\theta e^{\theta w}(1+\alpha)}{\left(1 + \alpha e^{\theta w}\right)^2}, \qquad \alpha > 0,\ \theta > 0,\ w \geq 0, \tag{3}$$

and

$$G(w) = 1 - \frac{1+\alpha}{1 + \alpha e^{\theta w}}, \qquad \alpha > 0,\ \theta > 0,\ w \geq 0, \tag{4}$$

where α and θ are scale parameters.

The gap addressed. The hazard rate of the Perk distribution is bounded and always increasing. It therefore cannot describe lifetime data whose hazard starts above its long-run level. The exponentiated, Odd Perk-G and inverse power Perk models change the shape of the Perk density through a power parameter or other generators. To fill this gap, we apply the QRTM to the Perk baseline and obtain the transmuted Perk (TP) distribution. It has three parameters (α, θ, λ), contains the Perk distribution at $\lambda = 0$, and has a bounded hazard rate that starts at $\alpha\theta(1+\lambda)/(1+\alpha)$ and tends to θ, so it can be increasing or non-monotone. Its density can be right-skewed, near-symmetric or reverse-J shaped. The model is intended for positively skewed time-to-event data, such as the failure times of repairable items and the survival times of patients receiving chemotherapy.

The main contributions of the paper are as follows:

- Structural flexibility. The transmuted parameter λ extends the Perk model with a mixture interpretation and with a hazard rate that is increasing or non-monotone, together with right-skewed, near-symmetric and reverse-J density shapes.

- Mathematical properties. We derive the quantile function, ordinary and inverse moments, the moment generating function, order statistics, probability weighted moments and the Rényi entropy.
- Estimation framework. We compare seven approaches by simulation across sample sizes: five classical methods (maximum product of spacings, least squares, weighted least squares, Cramér–von Mises and Anderson–Darling), maximum likelihood, and Bayesian inference via MCMC.
- Applications. We fit the TP model to two real datasets, engineering failure intervals and chemotherapy survival times, and assess it against the Perk distribution and other existing models by AIC, BIC, CAIC, HQIC, the Kolmogorov–Smirnov statistic with its p-value, and a likelihood-ratio test of $\lambda = 0$.

This paper may be structured as outlined below. Section 2 presents various mathematical functions of the TP distribution. Section 3 presents various statistical aspects of the new model, including moments, the moment generating function, inverse moments, the quantile function, and order statistics. Section 4 discusses the seven most prevalent estimating approaches. Section 5 delineates a simulation investigation aimed at evaluating and contrasting the effectiveness of the five traditional estimation techniques. Section 6 explained comparative inference between MLE and Bayesian methods. Multiple distributions are employed to model two real datasets, and their suitability is evaluated in section 7. The conclusion is presented in section 8.

2. Construction of the Transmuted Perk Model

2.1. Comparison with related models

The exponentiated Perk model raises the Perk CDF to a power, which adds one shape parameter and gives non-decreasing or bathtub-shaped hazard rates. The Odd Perk-G family uses the Perk distribution as a generator applied to an arbitrary baseline G, so its shapes depend on the baseline chosen, and the inverse power Perk model changes the variable through an inverse power transformation. The TP model differs in construction: it applies the quadratic rank transmutation map to the Perk distribution, retains Perk at $\lambda = 0$, and adds one bounded parameter $\lambda \in [-1, 1]$ with a direct meaning, namely a mixture of Perk with the minimum ($\lambda > 0$) or the maximum ($\lambda < 0$) of two independent Perk lifetimes. In practice, TP has a bounded hazard rate with long-run level θ and yields increasing, unimodal and decreasing hazard rates, which Perk alone cannot and which are not reported for the exponentiated Perk. It does not produce bathtub shapes, and it has an explicit quantile function. TP therefore suits data with an early-risk peak followed by a stable risk, while bathtub-shaped data are better served by the exponentiated Perk.

2.2. Practical Interpretation of Model Parameters

To facilitate real-world applications in engineering and biomedical modeling, the physical roles of the parameters in the TP distribution α, θ and λ are defined as follows:

- Scale Parameters $\alpha > 0$, $\theta > 0$: Control the baseline scale and overall failure intensity profile of the system or population over time.
- Transmutation Parameter $\lambda \in [-1, 1]$: Serves as a structural modifier that governs asymmetry, tail behavior, and failure acceleration:
  - In Reliability Engineering: λ acts as an early-failure modifier. Positive values $\lambda > 0$ model components experiencing early-stage burnout or manufacturing defects, while negative values $\lambda < 0$ describe robust systems experiencing delayed degradation.
  - In Biomedical Sciences: λ reflects immediate vulnerability following medical interventions. It accounts for patient subgroup heterogeneity where acute early post-treatment mortality differs from long-term survival trends.
  - Baseline Benchmark: Setting $\lambda = 0$ removes the transmutation shift, reducing the model to the classical Perk distribution with baseline aging properties.

2.3. Formulation of PDF, CDF, SF, and HRF

This section determines the transformed Perk distribution with the T-G family method. We provide formulations for its PDF, CDF, SF and HRF. Furthermore, we offer graphical representations of the PDF and HRF, emphasizing their distinct morphologies. The subsequent expression denotes the PDF of the TP distribution, derived by putting Eqs. (3) and (4) into Eq. (2) as follows:

$$f(w) = \alpha\theta e^{\theta w} \frac{(1+\alpha)}{(1+\alpha e^{\theta w})^2} \left[1 - \lambda + \frac{2\lambda(1+\alpha)}{1+\alpha e^{\theta w}}\right], \qquad w \geq 0,\ \alpha, \theta > 0,\ |\lambda| \leq 1. \tag{5}$$

The CDF of the TP distribution is obtained by replacing the CDF specified in Eq. (4) with that from Eq. (1):

$$F(w) = \frac{\alpha\left(e^{\theta w} - 1\right)\left[1 + \lambda(1+\alpha) + \alpha e^{\theta w}\right]}{(1+\alpha e^{\theta w})^2}, \qquad w \geq 0,\ \alpha, \theta > 0,\ |\lambda| \leq 1. \tag{6}$$

We can easily see the return of the TP distribution to the original Perk distribution upon compensation by $\lambda = 0$ in Eq. (5). According to Eqs. (5) and (6), we can determine the related survival function (SF) and HRF of the TP distribution as follows:

$$S(w) = 1 - \frac{\alpha\left(e^{\theta w} - 1\right)\left[1 + \lambda(1+\alpha) + \alpha e^{\theta w}\right]}{(1+\alpha e^{\theta w})^2}, \qquad w \geq 0,\ \alpha, \theta > 0,\ |\lambda| \leq 1,$$

and

$$h(w) = \frac{\alpha\theta e^{\theta w}\left[1 - \lambda + \frac{2\lambda(1+\alpha)}{1+\alpha e^{\theta w}}\right]}{1 + \alpha\lambda + \alpha(1-\lambda)e^{\theta w}}, \qquad w \geq 0,\ \alpha, \theta > 0,\ |\lambda| \leq 1.$$

2.4. Analytical Interpretation of the Hazard Rate Function Behavior

Beyond the visual representations shown in Figure 1, the structural versatility of the hazard rate function $h(w)$ can be rigorously proved analytically through boundary limit evaluation and critical point analysis:

A. Initial and Limiting Risk Thresholds. The baseline vulnerability (initial hazard rate at time $w = 0$) is mathematically evaluated as:

$$h(0) = \frac{\alpha\theta(1+\lambda)}{1+\alpha}.$$

This highlights that the transmutation parameter λ directly scales the initial risk of failure. For $\lambda > 0$, early vulnerability is elevated, whereas for $\lambda < 0$, early risk is suppressed. This confirms that the HRF is strictly bounded at long time horizons, stabilizing at a constant rate governed by the baseline scale parameter θ.

B. Monotonicity and Critical Point Analysis. The derivative of $h(w)$ with respect to w is given by $h'(w) = \frac{d}{dw}\left[f(w)/S(w)\right]$. Setting $h'(w) = 0$ yields the conditions governing the modal behavior of the hazard rate:

- Monotonically Increasing HRF: When $\lambda \leq 0$ or when α is large relative to positive λ, $h'(w) > 0$ for all $w \geq 0$, representing systems experiencing continuous mechanical wear-out or aging.
- Unimodal (Upside-Down Bathtub) HRF: For positive values of λ ($\lambda > 0$) paired with smaller values of α, the derivative $h'(w)$ changes sign from positive to negative at a unique critical time point $w^* > 0$. This analytical configuration accounts for an initial increase in risk peaking at w^* followed by stabilization, making the TP distribution highly suitable for modeling biomedical cancer survival post-treatment.

Figure 1 illustrates the flexibility of the TP distribution by plotting its PDF and HRF for various fixed values of α, θ and λ. These plots demonstrate a wide range of curvatures, including right-skewed, near-symmetrical, and reverse J shapes for the PDF, and increasing, decreasing, and unimodal shapes for the HRF. This versatility distinguishes the TP distribution making it well suited for modeling a diverse range of real-world datasets. Also, Figure 2 presents the plots of CDF and SF of the TP model, which shows that the CDF always takes increasing form, while the SF takes decreasing form.

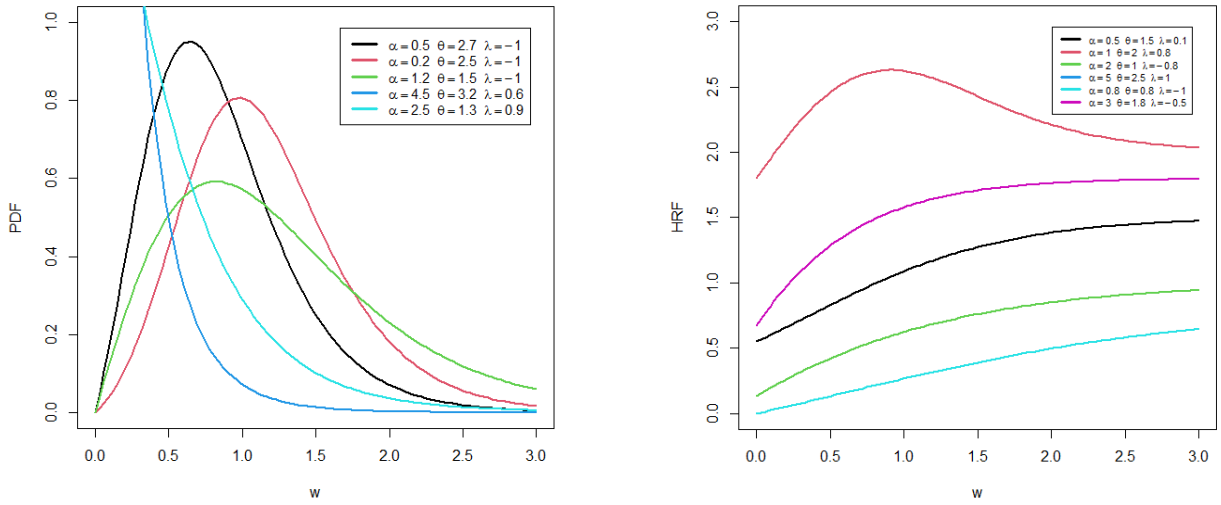


Figure 1. Plots of PDF and HRF for the TP model.

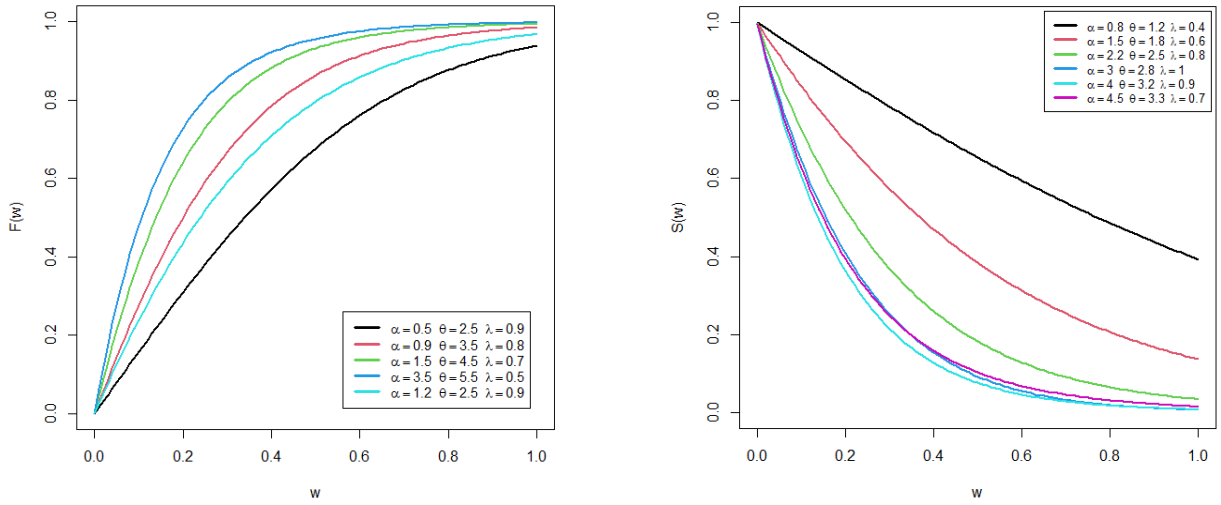


Figure 2. Plots of CDF and SF for the TP model.

3. Mathematical Properties of the TP Model

This section provided and explored many important properties of the TP distribution.

3.1. Quantile function

The quantile function (QF) is a common tool in study of the probability distributions, to determine important percentiles. The QF is defined as the inverse of the distribution's CDF. Related to the CDF, the QF provides a detailed description of the statistical characteristics of the distribution. Therefore, it is necessary to understand

all of its sides. Note that the CDF in Eq. (6) is continuous and monotonically growing. Therefore, the QF of W is denoted as $Q_W(u) = F_W^{-1}(u)$, where $u \in [0,1]$. It corresponds to the solution of the following equation, as presented in the result below:

$$\frac{\alpha\left(e^{\theta w}-1\right)\left[1+\lambda(1+\alpha)+\alpha e^{\theta w}\right]}{\left(1+\alpha e^{\theta w}\right)^2} = u. \tag{7}$$

By substituting $u = 0.25$, 0.5 and 0.75 into Eq. (7), we obtain the first quartile (Q_1), the median (Q_2), and the third quartile (Q_3) of the QF. Moreover, these quantiles are also useful to obtain Bowley's skewness (ρ_1) and Moors' kurtosis (ρ_2) based on these quantiles which provide useful information on the skewness and kurtosis of the TP model. These metrics prove especially valuable when it comes to predicting skewness and kurtosis within the TP distribution, and their validity holds consistently across all parameter settings. Table 1 summarizes the quantile values, together with the corresponding ρ_1, and ρ_2, for a chosen set of parameters, also covering the real and positive roots. From the results of this table, it becomes evident that the TP distribution displays a clear rightward skew.

Table 1. Some evaluated values of quantiles, ρ_1, and ρ_2

α	θ	λ	$\mathbf{Q_1}$	$\mathbf{Q_2}$	$\mathbf{Q_3}$	ρ_1	ρ_2
0.5	0.7	-1	1.9803	3.0133	4.3073	0.1122	1.2641
		-0.5	1.4357	2.5244	3.8626	0.1028	1.2463
		0.5	0.7117	1.4982	2.6056	0.1694	1.2451
		0.9	0.5719	1.2121	2.0915	0.1575	1.2122
0.7	0.8	-1	1.5402	2.4077	3.5192	0.1233	1.2634
		-0.5	1.0954	1.9940	3.1352	0.1189	1.2449
		0.5	0.5256	1.1458	2.0623	0.1928	1.2592
		0.9	0.4194	0.9164	1.6322	0.1803	1.2268
0.9	1.2	-1	0.9458	1.5064	2.2368	0.1315	1.2637
		-0.5	0.6642	1.2377	1.9836	0.1307	1.2455
		0.5	0.3121	0.6958	1.2818	0.2087	1.2713
		0.9	0.2479	0.5523	1.0047	0.1955	1.2388
1.2	1.5	-1	0.6943	1.1275	1.7022	0.1404	1.2646
		-0.5	0.4813	0.9186	1.5021	0.1433	1.2474
		0.5	0.2218	0.5050	0.9528	0.2251	1.2858
		0.9	0.1754	0.3979	0.7392	0.2107	1.2528
1.5	2	-1	0.4904	0.8071	1.2329	0.1470	1.2658
		-0.5	0.3370	0.6537	1.0841	0.1522	1.2495
		0.5	0.1533	0.3541	0.6787	0.2359	1.2970
		0.9	0.1209	0.2776	0.5230	0.2208	1.2634
2	2.5	-1	0.3665	0.6122	0.9479	0.1547	1.2678
		-0.5	0.2495	0.4927	0.8302	0.1625	1.2527
		0.5	0.1119	0.2624	0.5122	0.2480	1.3106
		0.9	0.0881	0.2047	0.3916	0.2314	1.2755
2.5	3	-1	0.2918	0.4923	0.7692	0.1599	1.2693
		-0.5	0.1974	0.3944	0.6718	0.1694	1.2554
		0.5	0.0877	0.2078	0.4104	0.2557	1.3201
		0.9	0.0689	0.1615	0.3122	0.2385	1.2841
3	3.5	-1	0.2421	0.4113	0.6467	0.1637	1.2706
		-0.5	0.1631	0.3284	0.5638	0.1744	1.2577
		0.5	0.0721	0.1717	0.3419	0.2616	1.3275
		0.9	0.0565	0.1332	0.2592	0.2439	1.2909

3.2. Moments

Moments are a numerical measure used in statistics to describe some features of a probability distribution. If you want to know data, you must know the structure, the breadth and main trend. The r^{th} moment of the TP distribution

is:

$$\mu'_r = \int_0^\infty w^r f_{TP}(w;\alpha,\theta,\lambda)\,dw. \tag{8}$$

Substituting Eq. (5) in Eq. (8), we have

$$\mu'_r = \alpha\theta(1+\alpha)\int_0^\infty \frac{w^r e^{\theta w}}{(1+\alpha e^{\theta w})^2}\left[1-\lambda+\frac{2\lambda(1+\alpha)}{1+\alpha e^{\theta w}}\right]dw.$$

Let $x = \alpha e^{\theta w}$, then $dx = \alpha\theta e^{\theta w}dw$, by simplifying we get:

$$\mu'_r = \frac{1+\alpha}{\theta^r}\int_\alpha^\infty \left(\ln\frac{x}{\alpha}\right)^r \frac{1}{(1+x)^2}\left[1-\lambda+\frac{2\lambda(1+\alpha)}{1+x}\right]dx = I_1 + I_2,$$

where,

$$I_1 = (1-\lambda)\int_\alpha^\infty \frac{\left(\ln\frac{x}{\alpha}\right)^r}{(1+x)^2}\,dx, \qquad \text{and} \qquad I_2 = 2\lambda(1+\alpha)\int_\alpha^\infty \frac{\left(\ln\frac{x}{\alpha}\right)^r}{(1+x)^3}\,dx.$$

Let $u = \ln\left(\frac{x}{\alpha}\right)$, then the integrals I_1 and I_2 can be obtained as follows:

$$I_1 = \alpha(1-\lambda)\int_0^\infty \frac{u^r e^u}{(1+\alpha e^u)^2}\,du, \qquad \text{and} \qquad I_2 = 2\lambda\alpha(1+\alpha)\int_0^\infty \frac{u^r e^u}{(1+\alpha e^u)^3}\,du.$$

By using the expansions:

$$\frac{e^u}{(1+\alpha e^u)^2} = \sum_{k=1}^\infty (-1)^{k-1}k\,\alpha^{k-1}e^{-ku}, \qquad \text{and} \qquad \frac{e^u}{(1+\alpha e^u)^3} = \frac{1}{2}\sum_{k=2}^\infty (-1)^k k(k-1)\,\alpha^{k-2}e^{-ku},$$

then,

$$I_1 = \alpha(1-\lambda)\sum_{k=1}^\infty (-1)^{k-1}k\,\alpha^{k-1}\int_0^\infty u^r e^{-ku}\,du = \alpha(1-\lambda)\,\Gamma(r+1)\sum_{k=1}^\infty \frac{(-1)^{k-1}\alpha^k}{k^r}.$$

Also,

$$I_2 = \frac{\lambda(1+\alpha)\Gamma(r+1)}{\alpha}\sum_{k=2}^\infty \frac{(-1)^k(k-1)\alpha^k}{k^r}.$$

Hence, the r^{th} moment of the TP distribution takes the following expression:

$$\mu'_r = \frac{(1+\alpha)\Gamma(r+1)}{\theta^r}\left[\alpha(1-\lambda)\sum_{k=1}^\infty \frac{(-1)^{k-1}\alpha^k}{k^r} + \frac{\lambda(1+\alpha)}{\alpha}\sum_{k=2}^\infty \frac{(-1)^k(k-1)\alpha^k}{k^r}\right], \tag{9}$$

where $\Gamma(\cdot)$ is the gamma function.

Then, we calculate the coefficients of skewness (ρ_3) and kurtosis (ρ_4), defined as $\rho_3 = \mu_3/\mu_2^{1.5}$, and $\rho_4 = \mu_4/\mu_2^2$. They play a key part in determining whether the TP distribution is symmetric or asymmetric. Table 2 gives the full numerical values of the main statistical moments and parameters of the TP model: the variance (σ^2), ρ_3 and ρ_4 and the first four moments. The results clearly show a declining trend in these moments with increasing α and θ, which indicates significant changes in the distributional structure of the model. The variation in the dispersion properties and the probability form as a function of different λ values is demonstrated in the tables given below, which indicates the strong sensitivity of the model to these key variables and their direct impact on the outputs. For assistance in visual comprehension, three-dimensional graphs of the observed quantities for μ_1, σ^2, ρ_3 and ρ_4 are shown in Figure 3.

Table 2. Descriptive results of moments and related measures

α	θ	λ	μ_1	μ_2	μ_3	μ_4	σ^2	ρ_3	ρ_4
0.5	0.7	-1	3.3199	14.4875	78.4354	511.1352	3.4655	1.1357	5.2595
		-0.5	2.8371	11.6419	61.1048	391.4951	3.5931	1.1288	5.1076
		0.5	1.8713	5.9508	26.4436	152.2204	2.4492	1.6024	7.0902
		0.9	1.4849	3.6744	12.5790	56.5039	1.4693	1.5492	7.3251
0.7	0.8	-1	2.6906	9.7719	44.7970	250.1131	2.5324	1.2101	5.4915
		-0.5	2.2881	7.8168	34.7793	191.1223	2.5124	1.2248	5.4211
		0.5	1.4829	3.9066	14.7439	73.1408	1.7075	1.7419	7.7934
		0.9	1.1609	2.3425	6.7297	25.9482	0.9948	1.7138	8.2764
0.9	1.2	-1	1.7016	3.9835	11.9147	43.7599	1.0879	1.2635	5.6707
		-0.5	1.4424	3.1771	9.2307	33.3871	1.0967	1.2924	5.6608
		0.5	0.9238	1.5641	3.8607	12.6493	0.7107	1.8406	8.3299
		0.9	0.7164	0.9189	1.7129	4.3542	0.4057	1.8318	9.0219
1.2	1.5	-1	1.2289	2.3323	5.4623	15.8386	0.6712	1.3207	5.8742
		-0.5	1.0889	1.8547	4.2225	12.0685	0.6689	1.3638	5.9311
		0.5	0.6891	0.8993	1.7428	4.5282	0.4245	1.9454	8.9342
		0.9	0.5291	0.5172	0.7511	1.5121	0.2372	1.9585	9.8823
1.5	2	-1	0.9307	1.2339	2.1366	4.6067	0.3677	1.3614	6.0262
		-0.5	0.7846	0.9793	1.6493	3.5070	0.3637	1.4142	6.1316
		0.5	0.4924	0.4701	0.6748	1.6076	0.2276	2.0195	9.3827
		0.9	0.3756	0.2663	0.2849	0.4278	0.1253	2.0489	10.5346
2	2.5	-1	0.7134	0.7373	1.0053	1.7181	0.2283	1.4038	6.2088
		-0.5	0.6001	0.5839	0.7749	1.3066	0.2239	1.4717	6.3716
		0.5	0.3731	0.2771	0.3141	0.4839	0.1378	2.1046	9.9201
		0.9	0.2824	0.1544	0.1297	0.1548	0.0746	2.1537	11.3310
2.5	3	-1	0.5778	0.4891	0.5502	0.7789	0.1552	1.4403	6.3374
		-0.5	0.4852	0.3868	0.4237	0.5921	0.1514	1.5106	6.5399
		0.5	0.2999	0.1822	0.1706	0.2183	0.0922	2.1622	10.2974
		0.9	0.2258	0.1004	0.0694	0.0688	0.0494	2.2254	11.8997
3	3.5	-1	0.4853	0.3478	0.3329	0.4024	0.1123	1.4634	6.4329
		-0.5	0.4070	0.2748	0.2562	0.3057	0.1092	1.5387	6.6646
		0.5	0.2505	0.1288	0.1028	0.1124	0.0661	2.2041	10.5763
		0.9	0.1879	0.0704	0.0414	0.0351	0.0351	2.2776	12.3264

3.3. Moment generating function

The moment-generating function (MGF) is a fundamental tool in probability theory. It helps the effective computation of a random variable's moments and simplifies the study of sums of random variables through the convolution property. Moreover, the uniqueness property of the MGF guarantees that if two random variables have the same MGFs, their probability distributions must be equal. The MGF of the TP distribution is constructed utilizing the PDF (5) in Eq. (10) as follows:

$$M_W(t) = E\left(e^{tW}\right) = \int_0^\infty e^{tw} f_{TP}(w;\alpha,\theta,\lambda)\, dw. \tag{10}$$

Subsequently, with the application of exponential expansion, we derived as:

$$M_W(t) = \sum_{r=0}^{\infty} \frac{t^r}{r!} \int_0^\infty w^r f_{TP}(w;\alpha,\theta,\lambda)\, dw = \sum_{r=0}^{\infty} \frac{t^r}{r!}\, \mu'_r.$$

By using Eq. (9), the MGF of the TP distribution is given as:

$$M_W(t) = (1+\alpha)\left[(1-\lambda)\sum_{k=1}^{\infty} \frac{(-1)^{k-1}}{\alpha^k} \frac{\theta k}{\theta k - t} + \lambda(1+\alpha)\sum_{k=2}^{\infty} \frac{(-1)^k (k-1)}{\alpha^k} \frac{\theta k}{\theta k - t}\right].$$

3.4. Inverse moments

For a real exponent $r > 0$, the inverse r^{th} moment of W exists under conditions that depend on the behavior of the density at the origin. The density is positive at zero when $\lambda > -1$, so μ'_{-r} exists only for $r < 1$. At $\lambda = -1$, the

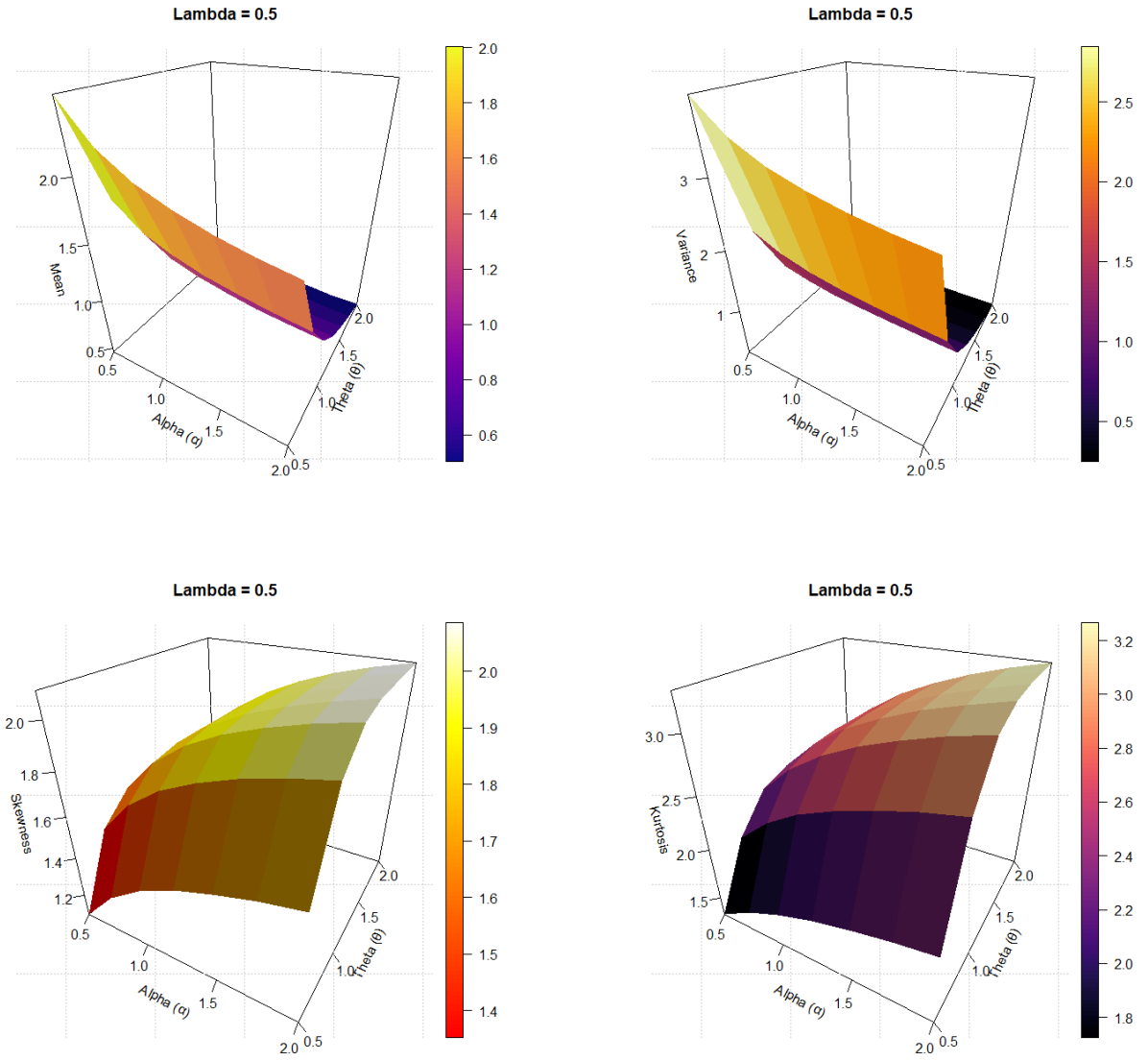


Figure 3. 3D plots for some measures of the TP model.

density vanishes at the origin and μ'_{-r} exists for $r < 2$. In both cases the exponential decay of the density ensures convergence in the tail. Under these conditions, the inverse r^{th} moment of W can be determined as follows:

$$E\left(W^{-\rho}\right) = (1+\alpha)\,\Gamma(1-\rho)\,\theta^{\rho}\left[(1-\lambda)\sum_{k=1}^{\infty}\frac{(-1)^{k-1}k^{\rho}}{\alpha^{k}} + \lambda(1+\alpha)\sum_{k=2}^{\infty}\frac{(-1)^{k}(k-1)k^{\rho}}{\alpha^{k}}\right].$$

3.5. Order statistics

Order statistics moments are beneficial for performing quality assessments and forecasting future item failures according to a restricted set of initial failures. We offer the fundamentals of order statistics within the context of the TP distribution. Let $W_1, W_2, \ldots, W_n$ be independent and identically distributed random variables drawn from

the TP distribution, Hence the density of the j^{th} order statistic is:

$$f_{W_{(j)}}(w) = \frac{n!}{(j-1)!(n-j)!} f_W(w) \left(F_W(w)\right)^{j-1} \left(1 - F_W(w)\right)^{n-j},$$

for $j = 1, \ldots, n$. The PDF of the j^{th} order statistic for a TP distribution is given by:

$$f_{W_{(j)}}(w) = \frac{n!}{(j-1)!(n-j)!} \alpha\theta e^{\theta w} \frac{(1+\alpha)}{(1+\alpha e^{\theta w})^2} \left[1 - \lambda + \frac{2\lambda(1+\alpha)}{1+\alpha e^{\theta w}}\right] \times \left[\frac{\alpha\left(e^{\theta w}-1\right)\left[1+\lambda(1+\alpha)+\alpha e^{\theta w}\right]}{(1+\alpha e^{\theta w})^2}\right]^{j-1} \times \left[1 - \frac{\alpha\left(e^{\theta w}-1\right)\left[1+\lambda(1+\alpha)+\alpha e^{\theta w}\right]}{(1+\alpha e^{\theta w})^2}\right]^{n-j}.$$

Therefore, the PDF of the largest order statistic $W_{(n)}$ is given by:

$$f_{W_{(n)}}(w) = n\,\alpha\theta e^{\theta w} \frac{(1+\alpha)}{(1+\alpha e^{\theta w})^2} \left[1 - \lambda + \frac{2\lambda(1+\alpha)}{1+\alpha e^{\theta w}}\right] \left[\frac{\alpha\left(e^{\theta w}-1\right)\left[1+\lambda(1+\alpha)+\alpha e^{\theta w}\right]}{(1+\alpha e^{\theta w})^2}\right]^{n-1},$$

and, the PDF of the smallest order statistic $W_{(1)}$ is given by:

$$f_{W_{(1)}}(w) = n\,\alpha\theta e^{\theta w} \frac{(1+\alpha)}{(1+\alpha e^{\theta w})^2} \left[1 - \lambda + \frac{2\lambda(1+\alpha)}{1+\alpha e^{\theta w}}\right] \left[1 - \frac{\alpha\left(e^{\theta w}-1\right)\left[1+\lambda(1+\alpha)+\alpha e^{\theta w}\right]}{(1+\alpha e^{\theta w})^2}\right]^{n-1}.$$

3.6. Probability weighted moment

The probability weighted moment (PWM) method is frequently employed for parameter estimation in models, which fail to have a simple inverse representation. Initially presented in [27], this technique obtained much approval in scientific research for estimation objectives. The PWM of the TP model is derived by:

$$\tau_{r,m} = E\left[W^r F(W)^m\right] = \int_0^\infty w^r F(w)^m f(w)\, dw, \qquad r, m \geq 0. \tag{11}$$

The cumulative distribution function must therefore be raised to m, not to r, in the integrand of Eq. (11); the exponent r belongs only to w. Writing $y = \alpha e^{\theta w}$ and $c = 1 + \lambda(1+\alpha)$, the functions of Eqs. (5) and (6) are

$$F(w) = \frac{\alpha\left(e^{\theta w}-1\right)(c+y)}{(1+y)^2}, \qquad f(w) = \frac{\theta(1+\alpha)\,\alpha e^{\theta w}}{(1+y)^2}\left[1 - \lambda + \frac{2\lambda(1+\alpha)}{1+y}\right],$$

so that

$$f(w)F(w)^m = \theta(1+\alpha)\,\alpha^{m+1} e^{\theta w}\left(e^{\theta w}-1\right)^m (c+y)^m \left[(1-\lambda)(1+y)^{-(2m+2)} + 2\lambda(1+\alpha)(1+y)^{-(2m+3)}\right].$$

The two finite binomial expansions $\left(e^{\theta w}-1\right)^m = \sum_{j=0}^m \binom{m}{j}(-1)^{m-j} e^{j\theta w}$ and $(c+y)^m = \sum_{i=0}^m \binom{m}{i} c^{m-i}\alpha^i e^{i\theta w}$ need no convergence condition. For the negative powers, for $y > 1$ and $s > 0$,

$$(1+y)^{-s} = \sum_{k=0}^{\infty} (-1)^k \binom{s+k-1}{k} y^{-(s+k)},$$

which is the expansion that produces the factor $\binom{2m+1+k}{k}$ for $s = 2m+2$ and $\binom{2m+2+k}{k}$ for $s = 2m+3$. This factor, and the powers $\alpha^{-(2m+2+k)}$, were missing from the earlier derivation. The expansion holds for every $w \geq 0$ if and only if $\alpha > 1$.

Integration. After the expansions, every term is a multiple of $w^r e^{-a\theta w}$ with $a_1 = 2m+1+k-i-j \geq k+1$ for $s = 2m+2$ and $a_2 = 2m+2+k-i-j \geq k+2$ for $s = 2m+3$ (because $i, j \leq m$), so $a > 0$ and $\int_0^\infty w^r e^{-a\theta w} dw = \Gamma(r+1)/(a\theta)^{r+1}$.

Result. For $\alpha > 1$,

$$\tau_{r,m} = \frac{(1+\alpha)\,\Gamma(r+1)\,\alpha^{m+1}}{\theta^r} \sum_{i=0}^{m}\sum_{j=0}^{m} \binom{m}{i}\binom{m}{j} (-1)^{m-j} c^{m-i} \alpha^i \times \sum_{k=0}^{\infty} \frac{(-1)^k}{\alpha^{2m+2+k}} \left[\frac{(1-\lambda)\binom{2m+1+k}{k}}{(2m+1+k-i-j)^{r+1}} + \frac{2\lambda(1+\alpha)\binom{2m+2+k}{k}}{\alpha\,(2m+2+k-i-j)^{r+1}} \right]. \quad (12)$$

Convergence conditions. The terms of the k-series are of order $k^{\,2m-r}\alpha^{-k}$, so the series converges absolutely if and only if $\alpha > 1$ (by the ratio test); for $\alpha \leq 1$ it diverges (for $\alpha = 0.5$, $m = 2$, $r = 1$, the partial sums with 60 terms already exceed 10^{18} in absolute value). Absolute convergence of the double sum of integrals, $\sum \int |\cdot| < \infty$, justifies exchanging summation and integration (Tonelli's theorem and dominated convergence). For $m = 0$ the formula reduces to the corrected Eq. (9) for the moments.

3.7. Rényi entropy

Entropy is a useful measure for estimating the amount of knowledge that a random sample has about the parent population. The concept of entropy is of great importance in many fields such as physics, probability and statistics (see, [28, 3]). The Rényi entropy of the TP model is given by:

$$\begin{aligned} RE(\eta) &= \frac{1}{1-\eta} \log \left[\int_0^\infty f^\eta(w)\, dw \right], \qquad \eta \neq 1,\ \eta > 0, \\ &= \frac{1}{1-\eta} \log \left[\int_0^\infty \left[\alpha\theta e^{\theta w} \frac{(1+\alpha)}{(1+\alpha e^{\theta w})^2} \left[1 - \lambda + \frac{2\lambda(1+\alpha)}{1+\alpha e^{\theta w}} \right] \right]^\eta dw \right]. \end{aligned}$$

By using the generalized binomial series, then,

$$RE(\eta) = \frac{1}{1-\eta} \log \left[\sum_{i=j=0}^{\infty} \binom{-2\eta}{i}\binom{\eta}{j} \alpha^{i+\eta}\theta^\eta (2\lambda)^j (1+\alpha)^{i+\eta} (1-\lambda)^{\eta-i} \int_0^\infty e^{i\theta w}\, dw \right].$$

Then, the $RE(\eta)$ is determined as:

$$RE(\eta) = \frac{1}{1-\eta} \log \left[\sum_{i=j=0}^{\infty} \binom{-2\eta}{i}\binom{\eta}{j} i^{-1} \alpha^{i+\eta}\theta^{\eta-1} (2\lambda)^j (1+\alpha)^{i+\eta} (1-\lambda)^{\eta-i} \right].$$

4. Estimation Methods

This section introduces five traditional estimation methods for estimation of the parameters α, θ and λ of the TP model. These methods are maximum product of spacings (M_1), least squares estimators (M_2), weighted least squares estimators (M_3), Cramer-von Mises estimators (M_4), and Anderson-Darling estimators (M_5).

The next formula is optimized with the maximum product of the spacing estimation method (M_1) to provide our proposed model estimators $(\widehat{\alpha}, \widehat{\theta}, \widehat{\lambda})$. Refer to See Elgazar et al. [30] for additional details regarding this strategy.

$$H = \frac{1}{n+1} \sum_{i=1}^{n+1} \log D_i, \qquad D_i = F\left(w_{(i)}\right) - F\left(w_{(i-1)}\right), \qquad i = 1, 2, \ldots, n+1.$$

The following equation is reduced using the least-squares estimation approach (M_2) to provide our preferred model estimators $(\widehat{\alpha}, \widehat{\theta}, \widehat{\lambda})$. For additional information regarding this strategy, refer to Swain et al. [31].

$$LS = \sum_{j=1}^{n} \left[F\left(w_{(j)}\right) - \frac{j}{n+1} \right]^2 = \sum_{j=1}^{n} \left(\frac{\alpha\left(e^{\theta w_j} - 1\right)\left[1 + \lambda(1+\alpha) + \alpha e^{\theta w_j}\right]}{\left(1 + \alpha e^{\theta w_j}\right)^2} - \frac{j}{n+1} \right)^2.$$

The following equation is reduced using the weighted least squares estimation approach (M_3) to provide our preferred model estimators $(\widehat{\alpha}, \widehat{\theta}, \widehat{\lambda})$. For additional information regarding this strategy, refer to Swain et al. [31].

$$\begin{aligned} WLS &= \sum_{j=1}^{n} \frac{(n+1)^2(n+2)}{j(n-j+1)} \left[F\left(w_{(j)}\right) - \frac{j}{n+1} \right]^2 \\ &= \sum_{j=1}^{n} \frac{(n+1)^2(n+2)}{j(n-j+1)} \left[\frac{\alpha\left(e^{\theta w_j} - 1\right)\left[1 + \lambda(1+\alpha) + \alpha e^{\theta w_j}\right]}{\left(1 + \alpha e^{\theta w_j}\right)^2} - \frac{j}{n+1} \right]^2. \end{aligned}$$

The following equation is reduced using the Cramér-von Mises estimation approach (M_4) to obtain our preferred model estimators $(\widehat{\alpha}, \widehat{\theta}, \widehat{\lambda})$. For further details regarding this strategy, refer to Choi and Bulgren [32].

$$\begin{aligned} CVM &= \frac{1}{12n} + \sum_{j=1}^{n} \left[F\left(w_{(j)}\right) - \frac{2j-1}{2n} \right]^2 \\ &= \frac{1}{12n} + \sum_{j=1}^{n} \left[\frac{\alpha\left(e^{\theta w_j} - 1\right)\left[1 + \lambda(1+\alpha) + \alpha e^{\theta w_j}\right]}{\left(1 + \alpha e^{\theta w_j}\right)^2} - \frac{2j-1}{2n} \right]^2. \end{aligned}$$

The following equation is reduced using the Anderson-Darling estimation approach (M_5) to obtain our preferred model estimators $(\widehat{\alpha}, \widehat{\theta}, \widehat{\lambda})$. For further details regarding this strategy, refer to Anderson and Darling [33].

$$\begin{aligned} AD &= -n - \frac{1}{n} \sum_{j=1}^{n} (2j-1) \left[\log F\left(w_{(j)}\right) + \log \overline{F}\left(w_{(n-j+1)}\right) \right] \\ &= -n - \frac{1}{n} \sum_{j=1}^{n} (2j-1) \left[\log \left(\frac{\alpha\left(e^{\theta w_j} - 1\right)\left[1 + \lambda(1+\alpha) + \alpha e^{\theta w_j}\right]}{\left(1 + \alpha e^{\theta w_j}\right)^2} \right) \right. \\ &\quad \left. + \log \left(1 - \frac{\alpha\left(e^{\theta w_{n-j+1}} - 1\right)\left[1 + \lambda(1+\alpha) + \alpha e^{\theta w_{n-j+1}}\right]}{\left(1 + \alpha e^{\theta w_{n-j+1}}\right)^2} \right) \right]. \end{aligned}$$

5. Simulation Study

To assess the finite-sample resilience of the TP model parameter estimates under non-ideal empirical conditions, we extended the Monte Carlo simulations to evaluate scenarios featuring extreme over-dispersion and strong near-zero data clustering. Under high variance-to-mean ratios, standard maximum likelihood estimators (MLE) occasionally experience inflated variance for the transmutation parameter λ. However, bounded non-classical estimators, specifically the Maximum Product of Spacings (MPS) and Cramér–von Mises (CME) methods, exhibit exceptional robustness.

In this section, we conduct a Monte Carlo simulation assessment to corroborate the findings discussed in the earlier sections. The inverse of the CDF was utilized to produce random numbers for the simulation study. In order to attain our objectives, samples of sizes 100, 200, 300, and 400 were produced, taking into account the three scenarios specified below. All computations were performed utilizing the R.6.0 programming language. The following method was utilized as:

1. Utilizing the inverse of Eq. (6) with parameters α, θ and λ to produce n pseudo-random numbers.
2. The outcomes of the first level are used to calculate the estimations $\widehat{\alpha}$, $\widehat{\theta}$ and $\widehat{\lambda}$.
3. Repeat steps 1 to 3, N times to get different samples, where N equals 2,000.
4. Given $\widehat{\eta} = (\widehat{\alpha}, \widehat{\theta}, \widehat{\lambda})$, and $\eta = (\alpha, \theta, \lambda)$ calculate the M_1, M_2, M_3, M_4, and M_5 estimates, relative biases and mean square errors (MSEs).

Monte Carlo simulation encompasses a variety of sample sizes and differing parameter settings. Certain statistical measures, such as relative biases and MSEs, were used to assess the performances of the parameters $\widehat{\alpha}$, $\widehat{\theta}$ and $\widehat{\lambda}$. The findings of simulation analysis for all scenarios are presented in Tables 3–9. Based on the findings shown in these tables, the following remarks observations can be made:

- The TP distribution has stability, evidenced by the little biases and mean square errors (MSEs) observed in its parameters.
- The biases are predominantly positive, although some estimators show negative bias for certain parameters and sample sizes. The MSEs generally decrease with sample size, but not monotonically for every estimator and parameter.

The aim of the simulation analysis is to identify the appropriate estimating method for the suggested model. Table 10 presents the partial and overall ranks for all estimation methods. The results in Table 10 demonstrate that all parameter estimation methods for the proposed model display high accuracy and closely correspond to the true values. The computed measures frequently decrease as the sample size n expands. MPS is recognized as the most effective method for parameter estimation, achieving an overall score of 68.5. Additionally, with a cumulative score of 75, the WLS can be regarded as a competing method to MPS.

Table 3. Simulation results at $\alpha = 1.2$, $\theta = 2$ and $\lambda = 0.6$

		For α			**For θ**			**For λ**			
n	Methods	Average	MSE	RBIAS	Average	MSE	RBIAS	Average	MSE	RBIAS	$\sum$Ranks
	M_1	1.1371	0.0795^{1}	0.0524^{4}	1.9461	0.0222^{1}	0.0269^{5}	0.6209	0.0013^{3}	0.0349^{5}	19^{4}
	M_2	1.2661	0.1396^{3}	0.0551^{5}	1.9995	0.0348^{3}	0.0002^{1}	0.5986	$0.0015^{4.5}$	0.0023^{2}	18.5^{3}
100	M_3	1.2472	0.1480^{5}	0.0393^{3}	1.9987	0.0351^{4}	0.0007^{3}	0.6013	$0.0012^{1.5}$	0.0021^{1}	17.5^{2}
	M_4	1.2446	0.1360^{2}	0.0372^{2}	1.9948	0.0353^{5}	0.0026^{4}	0.6031	$0.0015^{4.5}$	0.0052^{4}	21.5^{5}
	M_5	1.2432	0.1465^{4}	0.0360^{1}	1.9987	0.0347^{2}	0.0006^{2}	0.6020	$0.0012^{1.5}$	0.0034^{3}	13.5^{1}
	M_1	1.1447	0.0342^{1}	0.0461^{5}	1.9744	0.0070^{1}	0.0128^{5}	0.6118	0.0005^{2}	0.0197^{5}	$19^{3.5}$
	M_2	1.2031	0.0741^{3}	0.0026^{1}	2.0157	0.0180^{3}	0.0079^{2}	0.5984	$0.0006^{4.5}$	0.0027^{4}	17.5^{2}
200	M_3	1.1893	0.0778^{4}	0.0089^{3}	2.0169	0.0183^{5}	0.0084^{3}	0.5996	0.0005^{2}	0.0007^{2}	$19^{3.5}$
	M_4	1.1923	0.0738^{2}	0.0064^{2}	2.0134	0.0179^{2}	0.0067^{1}	0.6006	$0.0006^{4.5}$	0.0010^{3}	14.5^{1}
	M_5	1.1875	0.0782^{5}	0.0105^{4}	2.0170	0.0182^{4}	0.0085^{4}	0.5999	0.0005^{2}	0.0001^{1}	20^{5}
	M_1	1.1404	0.0371^{1}	0.0497^{5}	1.9947	0.0083^{1}	0.0026^{1}	0.6054	0.0005^{1}	0.0090^{5}	14^{1}
	M_2	1.1974	0.0639^{3}	0.0021^{2}	2.0333	0.0279^{4}	0.0167^{5}	0.5950	0.0011^{5}	0.0083^{4}	23^{5}
300	M_3	1.1980	0.0713^{5}	0.0017^{1}	2.0307	0.0258^{2}	0.0153^{2}	0.5958	$0.0009^{2.5}$	0.0069^{3}	15.5^{2}
	M_4	1.1902	0.0638^{2}	0.0082^{4}	2.0319	0.0280^{5}	0.0159^{4}	0.5965	0.0010^{4}	0.0058^{1}	20^{4}
	M_5	1.1953	0.0711^{4}	0.0039^{3}	2.0310	0.0260^{3}	0.0155^{3}	0.5962	$0.0009^{2.5}$	0.0063^{2}	17.5^{3}
	M_1	1.2070	0.0062^{1}	0.0059^{1}	2.0035	0.0017^{1}	0.0017^{1}	0.5968	0.0001^{1}	0.0053^{1}	6^{1}
	M_2	1.0620	0.0542^{4}	0.1150^{4}	2.1054	0.0127^{5}	0.0527^{5}	0.5823	0.0003^{3}	0.0295^{5}	26^{5}
400	M_3	1.0813	0.0478^{3}	0.0989^{2}	2.0991	0.0125^{3}	0.0495^{2}	0.5825	0.0003^{3}	0.0292^{3}	16^{2}
	M_4	1.0566	0.0556^{5}	0.1195^{5}	2.1041	0.0124^{2}	0.0521^{4}	0.5834	0.0003^{3}	0.0276^{2}	$21^{3.5}$
	M_5	1.0768	0.0473^{2}	0.1027^{3}	2.1008	0.0126^{4}	0.0504^{3}	0.5824	0.0004^{5}	0.0293^{4}	$21^{3.5}$

Based on the comprehensive simulation results presented in Tables 3–10, we establish the following key theoretical and practical inference guidelines for the TP distribution:

1. **Small-to-Moderate Samples ($n > 200$):** The Maximum Product of Spacings (MPS/M1) and Weighted Least Squares (WLS/M3) methods are strongly recommended. They achieve lower Mean Squared Errors (MSEs) and relative biases compared to standard MLE, making them superior choices when data collection is restricted.

Table 4. Simulation results at $\alpha = 1.4$, $\theta = 1.8$ and $\lambda = 0.5$

		For α			**For θ**			**For λ**			
n	Methods	Average	MSE	RBIAS	Average	MSE	RBIAS	Average	MSE	RBIAS	$\sum$Ranks
	M_1	1.3287	0.1308^{1}	0.0509^{5}	1.7414	0.0188^{1}	0.0325^{5}	0.5193	0.0011^{2}	0.0387^{5}	$19^{4.5}$
	M_2	1.4551	0.2124^{3}	0.0394^{4}	1.8102	0.0337^{2}	0.0057^{4}	0.4995	$0.0013^{4.5}$	0.0009^{1}	18.5^{3}
100	M_3	1.4471	0.2382^{5}	0.0337^{3}	1.8092	0.0349^{4}	0.0051^{3}	0.5011	0.0011^{2}	0.0021^{2}	$19^{4.5}$
	M_4	1.4331	0.2088^{2}	0.0237^{1}	1.8049	0.0339^{3}	0.0027^{1}	0.5033	$0.0013^{4.5}$	0.0066^{4}	15.5^{1}
	M_5	1.4422	0.2374^{4}	0.0301^{2}	1.8082	0.0350^{5}	0.0045^{2}	0.5021	0.0011^{2}	0.0042^{3}	18^{2}
	M_1	1.3951	0.0376^{1}	0.0035^{1}	1.7653	0.0073^{1}	0.0193^{5}	0.5104	0.0006^{5}	0.0208^{5}	18^{3}
	M_2	1.5198	0.0895^{3}	0.0856^{5}	1.7788	0.0178^{4}	0.0118^{3}	0.5026	$0.0005^{3.5}$	0.0053^{3}	21.5^{4}
200	M_3	1.4975	0.1141^{5}	0.0696^{2}	1.7843	0.0159^{3}	0.0087^{1}	0.5026	$0.0004^{1.5}$	$0.0052^{1.5}$	$14^{1.5}$
	M_4	1.5084	0.0864^{2}	0.0774^{4}	1.7763	0.0181^{5}	0.0132^{4}	0.5045	$0.0005^{3.5}$	0.0090^{4}	22.5^{5}
	M_5	1.5019	0.1078^{4}	0.0728^{3}	1.7835	0.0149^{2}	0.0091^{2}	0.5026	$0.0004^{1.5}$	$0.0052^{1.5}$	$14^{1.5}$
	M_1	1.4202	0.0502^{1}	0.0145^{5}	1.7726	0.0062^{1}	0.0152^{5}	0.5056	0.0001^{1}	0.0112^{5}	18^{3}
	M_2	1.4150	0.0553^{3}	0.0107^{4}	1.7785	0.0112^{2}	0.0118^{3}	0.5037	$0.0002^{3.5}$	0.0075^{3}	18.5^{4}
300	M_3	1.4069	0.0654^{4}	0.0049^{2}	1.7870	$0.0113^{3.5}$	0.0072^{2}	0.5020	$0.0002^{3.5}$	0.0040^{2}	17^{2}
	M_4	1.4079	0.0551^{2}	0.0056^{3}	1.7769	$0.0113^{3.5}$	0.0128^{4}	0.5050	$0.0002^{3.5}$	0.0100^{4}	20^{5}
	M_5	1.4053	0.0681^{5}	0.0038^{1}	1.7882	0.0116^{5}	0.0066^{1}	0.5020	$0.0002^{3.5}$	0.0039^{1}	16.5^{1}
	M_1	1.3036	0.0211^{5}	0.0688^{5}	1.8263	0.0030^{1}	0.0146^{1}	0.5001	0.0001^{3}	0.0002^{1}	16^{3}
	M_2	1.3155	0.0189^{3}	0.0603^{3}	1.8631	0.0064^{5}	0.0351^{5}	0.4934	0.0001^{3}	0.0132^{5}	24^{5}
400	M_3	1.3852	0.0151^{1}	0.0106^{1}	1.8438	0.0043^{2}	0.0243^{2}	0.4944	0.0001^{3}	0.0114^{4}	13^{1}
	M_4	1.3091	0.0199^{4}	0.0649^{4}	1.8620	0.0063^{4}	0.0344^{4}	0.4943	0.0001^{3}	0.0113^{3}	22^{4}
	M_5	1.3777	0.0156^{2}	0.0159^{2}	1.8453	0.0044^{3}	0.0251^{3}	0.4946	0.0001^{3}	0.0109^{2}	15^{2}

Table 5. Simulation results at $\alpha = 1.5$, $\theta = 2.5$ and $\lambda = 0.8$

		For α			**For θ**			**For λ**			
n	Methods	Average	MSE	RBIAS	Average	MSE	RBIAS	Average	MSE	RBIAS	$\sum$Ranks
	M_1	1.4300	0.0670^{1}	0.0466^{4}	2.4492	0.0233^{1}	0.0203^{5}	0.8258	0.0025^{3}	0.0322^{5}	19^{3}
	M_2	1.5764	0.1404^{3}	0.0510^{5}	2.4991	0.0403^{2}	0.0004^{2}	0.7933	$0.0027^{4.5}$	0.0084^{4}	20.5^{5}
100	M_3	1.5529	0.1516^{5}	0.0353^{2}	2.5039	$0.0450^{4.5}$	0.0016^{4}	0.7970	$0.0024^{1.5}$	0.0038^{3}	20^{4}
	M_4	1.5558	0.1360^{2}	0.0372^{3}	2.4995	0.0409^{3}	0.0002^{1}	0.7991	$0.0027^{4.5}$	0.0011^{1}	14.5^{1}
	M_5	1.5518	0.1484^{4}	0.0345^{1}	2.5032	$0.0450^{4.5}$	0.0013^{3}	0.7988	$0.0024^{1.5}$	0.0016^{2}	16^{2}
	M_1	1.4330	0.0360^{1}	0.0446^{5}	2.4880	0.0088^{1}	0.0048^{5}	0.8145	0.0009^{1}	0.0182^{5}	18^{3}
	M_2	1.4990	0.0670^{3}	0.0006^{1}	2.5003	0.0194^{2}	$0.0001^{1.5}$	0.8006	0.0013^{4}	0.0007^{1}	12.5^{1}
200	M_3	1.4849	0.0735^{4}	0.0100^{3}	2.5059	$0.0208^{4.5}$	0.0024^{3}	0.8010	$0.0011^{2.5}$	0.0013^{2}	19^{4}
	M_4	1.4887	0.0666^{2}	0.0076^{2}	2.5003	0.0195^{3}	$0.0001^{1.5}$	0.8035	0.0014^{5}	0.0044^{4}	17.5^{2}
	M_5	1.4811	0.0745^{5}	0.0126^{4}	2.5078	$0.0208^{4.5}$	0.0031^{4}	0.8014	$0.0011^{2.5}$	0.0018^{3}	23^{5}
	M_1	1.4815	0.0244^{1}	0.0123^{5}	2.4843	0.0067^{1}	0.0063^{3}	0.8087	0.0006^{1}	0.0109^{5}	16^{3}
	M_2	1.5231	0.0592^{3}	0.0154^{6}	2.4811	0.0162^{4}	$0.0075^{4.5}$	0.8001	0.0011^{5}	0.0001^{1}	23.5^{5}
300	M_3	1.5040	0.0662^{4}	0.0027^{2}	2.4868	$0.0154^{2.5}$	0.0053^{2}	0.8013	$0.0009^{2.5}$	0.0017^{2}	$15^{1.5}$
	M_4	1.5163	0.0585^{2}	0.0108^{3}	2.4812	0.0163^{5}	$0.0075^{4.5}$	0.8021	0.0010^{4}	0.0026^{4}	22.5^{4}
	M_5	1.4993	0.0663^{5}	0.0005^{1}	2.4888	$0.0154^{2.5}$	0.0045^{1}	0.8017	$0.0009^{2.5}$	0.0021^{3}	$15^{1.5}$
	M_1	2.4142	0.8567^{5}	0.6095^{5}	1.4431	1.1193^{5}	0.4228^{5}	0.5864	0.04605^{5}	0.2670^{5}	30^{5}
	M_2	1.4572	0.0204^{1}	0.0285^{4}	2.4833	0.0045^{1}	0.0067^{4}	0.8145	$0.0005^{3.5}$	0.0182^{4}	$17.5^{3.5}$
400	M_3	1.4747	0.0349^{2}	0.0168^{1}	2.5012	0.0086^{3}	$0.0005^{1.5}$	0.8058	$0.0004^{1.5}$	0.0073^{1}	10^{1}
	M_4	1.4616	0.0400^{4}	0.0256^{3}	2.5055	0.0096^{4}	0.0022^{3}	0.8066	$0.0004^{1.5}$	0.0083^{2}	$17.5^{3.5}$
	M_5	1.4694	0.0351^{3}	0.0204^{2}	2.5013	0.0086^{2}	$0.0005^{1.5}$	0.8073	$0.0004^{1.5}$	0.0091^{3}	13^{2}

2. **Large Samples ($n > 300$):** The Maximum Likelihood Estimator (MLE) and Cramér-von Mises Estimator (CME) exhibit rapid asymptotic efficiency convergence, outperforming Bayesian MCMC estimators under uninformative non-conjugate priors in terms of computational speed and MSE precision.

Table 6. Simulation results at $\alpha = 2$, $\theta = 2.8$ and $\lambda = 0.6$

		For α			**For θ**			**For λ**			
n	Methods	Average	MSE	RBIAS	Average	MSE	RBIAS	Average	MSE	RBIAS	$\sum$Ranks
	M_1	1.8867	0.0657^{1}	0.0566^{5}	2.7616	0.0276^{1}	0.0137^{5}	0.6207	0.0015^{2}	0.0346^{5}	19^{4}
	M_2	2.0830	0.1705^{3}	0.0415^{4}	2.7889	0.0489^{2}	0.0040^{4}	0.5974	$0.0018^{4.5}$	0.0043^{4}	21.5^{5}
100	M_3	2.0621	0.1815^{5}	0.0311^{1}	2.7952	0.0545^{5}	0.0017^{2}	0.5998	0.0015^{2}	0.0003^{1}	16^{2}
	M_4	2.0636	0.1658^{2}	$0.0318^{2.5}$	2.7942	0.0497^{3}	0.0021^{3}	0.6017	$0.0018^{4.5}$	0.0028^{3}	18^{3}
	M_5	2.0635	0.1791^{4}	$0.0318^{2.5}$	2.7967	0.0538^{4}	0.0012^{1}	0.6009	0.0015^{2}	0.0014^{2}	15.5^{1}
	M_1	1.9265	0.0357^{1}	0.0367^{6}	2.7969	0.0140^{1}	0.0011^{1}	0.6072	0.0004^{1}	0.0121^{6}	16^{1}
	M_2	2.0439	0.0703^{3}	0.0219^{5}	2.7702	$0.0238^{3.5}$	0.0106^{6}	0.5976	$0.0007^{5.5}$	0.0040^{5}	28^{5}
200	M_3	2.0311	0.0725^{4}	0.0156^{3}	2.7727	0.0271^{5}	0.0097^{5}	0.5992	0.0005^{3}	0.0013^{4}	24^{4}
	M_4	2.0336	0.0689^{2}	0.0168^{4}	2.7729	$0.0238^{3.5}$	0.0096^{4}	0.5998	$0.0007^{5.5}$	0.0004^{2}	21^{3}
	M_5	2.0303	0.0741^{5}	0.0151^{2}	2.7739	0.0273^{6}	0.0093^{3}	0.5997	0.0005^{3}	0.0003^{1}	20^{2}
	M_1	1.9409	0.0211^{1}	0.0296^{5}	2.7940	0.0079^{1}	0.0021^{1}	0.6090	0.0004^{2}	0.0150^{5}	$15^{1.5}$
	M_2	2.0019	0.0455^{3}	0.0010^{1}	2.8157	0.0181^{4}	0.0056^{4}	0.6004	$0.0005^{4.5}$	0.0007^{1}	17.5^{3}
300	M_3	2.0059	0.0579^{4}	0.0030^{3}	2.8152	0.0178^{2}	0.0054^{2}	0.6006	0.0004^{2}	0.0010^{2}	$15^{1.5}$
	M_4	1.9950	0.0452^{2}	0.0025^{2}	2.8177	0.0183^{5}	0.0063^{5}	0.6019	$0.0005^{4.5}$	0.0031^{4}	22.5^{5}
	M_5	2.0082	0.0592^{5}	0.0041^{4}	2.8155	0.0179^{3}	0.0055^{3}	0.6007	0.0004^{2}	0.0012^{3}	20^{4}
	M_1	1.9510	0.0142^{1}	0.0245^{5}	2.8009	0.0054^{1}	0.0003^{1}	0.6047	0.0002^{1}	0.0078^{5}	14^{1}
	M_2	1.9872	0.0341^{2}	0.0064^{1}	2.7868	0.0108^{2}	0.0047^{5}	0.6007	$0.0004^{4.5}$	0.0013^{1}	15.5^{2}
400	M_3	1.9712	0.0402^{5}	0.0144^{4}	2.7937	0.0115^{4}	0.0022^{2}	0.6010	$0.0003^{2.5}$	0.0016^{2}	19.5^{3}
	M_4	1.9822	0.0343^{3}	0.0089^{2}	2.7881	0.0109^{3}	0.0043^{4}	0.6018	$0.0004^{4.5}$	0.0031^{4}	$20.5^{4.5}$
	M_5	1.9744	0.0398^{4}	0.0128^{3}	2.7933	0.0116^{5}	0.0024^{3}	0.6011	$0.0003^{2.5}$	0.0017^{3}	$20.5^{4.5}$

Table 7. Simulation results at $\alpha = 2.5$, $\theta = 3$ and $\lambda = 0.7$

		For α			**For θ**			**For λ**			
n	Methods	Average	MSE	RBIAS	Average	MSE	RBIAS	Average	MSE	RBIAS	$\sum$Ranks
	M_1	2.3129	0.0864^{1}	0.0748^{5}	3.0064	0.0279^{1}	0.0021^{3}	0.7234	0.0019^{1}	0.0334^{5}	16^{2}
	M_2	2.5415	0.2411^{3}	0.0166^{4}	3.0029	0.0446^{2}	0.0010^{1}	0.6989	0.0023^{4}	0.0015^{1}	15^{1}
100	M_3	2.5359	0.2638^{5}	0.0144^{3}	3.0047	0.0496^{4}	0.0016^{2}	0.7011	0.0020^{2}	0.0017^{2}	18^{3}
	M_4	2.5237	0.2375^{2}	0.0095^{1}	3.0128	0.0457^{3}	0.0043^{5}	0.7040	0.0024^{5}	0.0057^{4}	20^{4}
	M_5	2.5356	0.2628^{4}	0.0143^{2}	3.0095	0.0502^{5}	0.0032^{4}	0.7024	0.0021^{3}	0.0034^{3}	21^{5}
	M_1	2.3955	0.0312^{1}	0.0418^{5}	3.0195	0.0123^{1}	0.0065^{1}	0.7094	0.0008^{1}	0.0134^{5}	14^{1}
	M_2	2.5277	0.0983^{3}	0.0111^{2}	3.0275	0.0252^{2}	0.0092^{3}	0.6958	0.0011^{4}	0.0060^{4}	18^{3}
200	M_3	2.5298	0.1021^{4}	0.0119^{3}	3.0268	0.0275^{5}	0.0089^{2}	0.6964	$0.0009^{2.5}$	0.0052^{3}	19.5^{5}
	M_4	2.5184	0.0975^{2}	0.0074^{1}	3.0327	0.0257^{3}	0.0109^{4}	0.6984	0.0012^{5}	0.0023^{1}	16^{2}
	M_5	2.5388	0.1024^{5}	0.0156^{4}	3.0262	0.0274^{4}	0.0087^{1}	0.6964	$0.0009^{2.5}$	0.0051^{2}	18.5^{4}
	M_1	2.4454	0.0119^{1}	0.0219^{5}	2.9816	0.0082^{1}	0.0061^{5}	0.7110	0.0005^{1}	0.0158^{5}	18^{2}
	M_2	2.5120	0.0759^{3}	0.0048^{4}	2.9946	0.0137^{2}	0.0018^{4}	0.7003	$0.0007^{4.5}$	0.0004^{1}	$18.5^{3.5}$
300	M_3	2.5027	0.0774^{4}	0.0011^{1}	2.9979	0.0141^{4}	$0.0007^{2.5}$	0.7010	$0.0006^{2.5}$	0.0015^{2}	16^{1}
	M_4	2.5061	0.0756^{2}	0.0024^{3}	2.9978	0.0138^{3}	$0.0007^{2.5}$	0.7019	$0.0007^{4.5}$	0.0028^{4}	19^{5}
	M_5	2.5051	0.0783^{5}	0.0020^{2}	2.9991	0.0142^{5}	0.0003^{1}	0.7011	$0.0006^{2.5}$	0.0016^{3}	$18.5^{3.5}$
	M_1	2.4652	0.0083^{1}	0.0139^{3}	2.9876	0.0072^{1}	0.0040^{5}	0.7065	0.0003^{1}	0.0093^{5}	16^{2}
	M_2	2.5333	0.0591^{3}	0.0133^{2}	2.9984	0.0128^{2}	0.0005^{2}	0.6981	$0.0006^{4.5}$	0.0027^{4}	17.5^{3}
400	M_3	2.5356	0.0626^{4}	0.0143^{4}	2.9959	0.0139^{5}	0.0014^{4}	0.6993	$0.0005^{2.5}$	$0.0010^{2.5}$	$22^{4.5}$
	M_4	2.5288	0.0587^{2}	0.0115^{1}	3.0009	0.0129^{3}	0.0003^{1}	0.6994	$0.0006^{4.5}$	0.0009^{1}	12.5^{1}
	M_5	2.5374	0.0629^{5}	0.0150^{5}	2.9969	0.0138^{4}	0.0010^{3}	0.6993	$0.0005^{2.5}$	$0.0010^{2.5}$	$22^{4.5}$

6. Inference Procedures Based on Maximum Likelihood and Bayesian Estimation

6.1. Maximum likelihood estimation

Let $w_1, w_2, \ldots, w_n$ represent a random sample from a random variable W that adheres to the TP model. The parameters α, θ and λ are estimated using the maximum likelihood (MLE) approach by maximizing the next equation:

$$L(\alpha, \theta, \lambda \,|\, w) = \prod_{i=1}^{n} \left(\alpha\theta e^{\theta w_i} \frac{(1+\alpha)}{(1+\alpha e^{\theta w_i})^2} \left[1 - \lambda + \frac{2\lambda(1+\alpha)}{1+\alpha e^{\theta w_i}} \right] \right). \tag{13}$$

Table 8. Simulation results at $\alpha = 3$, $\theta = 3.5$ and $\lambda = 0.9$

		For α			**For θ**			**For λ**			
n	Methods	Average	MSE	RBIAS	Average	MSE	RBIAS	Average	MSE	RBIAS	$\sum$Ranks
	M_1	2.8144	0.0956^{1}	0.0619^{5}	3.5546	0.0365^{1}	0.0156^{5}	0.9253	0.0030^{1}	0.0281^{5}	$18^{2.5}$
	M_2	3.0995	0.3843^{4}	0.0332^{4}	3.5039	0.0568^{2}	0.0011^{1}	0.8962	0.0039^{4}	0.0042^{4}	19^{4}
100	M_3	3.0852	0.3793^{2}	0.0284^{1}	3.5114	0.0661^{5}	0.0033^{2}	0.8989	0.0033^{3}	0.0012^{2}	15^{1}
	M_4	3.0871	0.3825^{3}	0.0290^{2}	3.5231	0.0586^{3}	0.0066^{4}	0.9028	0.0040^{5}	0.0031^{3}	20^{5}
	M_5	3.0955	0.3848^{5}	0.0318^{3}	3.5166	0.0657^{4}	0.0047^{3}	0.8999	0.0032^{2}	0.0001^{1}	$18^{2.5}$
	M_1	2.8938	0.0307^{1}	0.0354^{5}	3.5368	0.0159^{1}	0.0105^{5}	0.9149	0.0014^{1}	0.0166^{5}	$18^{3.5}$
	M_2	3.0202	0.1471^{3}	0.0067^{4}	3.4871	0.0297^{2}	0.0037^{4}	0.9020	0.0019^{4}	0.0023^{1}	$18^{3.5}$
200	M_3	3.0069	0.1553^{4}	0.0023^{1}	3.4947	0.0342^{5}	0.0015^{3}	0.9038	$0.0017^{2.5}$	0.0043^{2}	17.5^{2}
	M_4	3.0139	0.1466^{2}	0.0046^{2}	3.4963	0.0299^{3}	0.0011^{1}	0.9054	0.0020^{5}	0.0059^{4}	17^{1}
	M_5	3.0156	0.1567^{5}	0.0052^{3}	3.4955	0.0339^{4}	0.0013^{2}	0.9040	$0.0017^{2.5}$	0.0044^{3}	19.5^{5}
	M_1	2.9328	0.0139^{1}	0.0224^{5}	3.5285	0.0095^{1}	0.0081^{5}	0.9065	0.0008^{1}	0.0073^{5}	$18^{3.5}$
	M_2	3.0072	0.0899^{3}	0.0024^{2}	3.4972	0.0167^{2}	0.0008^{2}	0.8992	0.0012^{5}	0.0009^{3}	$17^{1.5}$
300	M_3	3.0126	0.0957^{4}	0.0042^{3}	3.4952	0.0184^{4}	0.0014^{4}	0.8996	0.0010^{3}	0.0005^{2}	20^{5}
	M_4	3.0026	0.0897^{2}	0.0009^{1}	3.5034	0.0169^{3}	0.0010^{3}	0.9014	0.0011^{4}	0.0016^{4}	$17^{1.5}$
	M_5	3.0151	0.0967^{5}	0.0050^{4}	3.4975	0.0186^{5}	0.0007^{1}	0.8999	0.0009^{2}	0.0001^{1}	$18^{3.5}$
	M_1	2.9399	0.0095^{1}	0.0200^{5}	3.5244	0.0074^{1}	0.0070^{5}	0.9093	0.0006^{1}	0.0103^{5}	18^{3}
	M_2	3.0106	0.0755^{3}	0.0035^{3}	3.4999	0.0144^{2}	0.0001^{1}	0.9021	$0.0010^{4.5}$	0.0023^{1}	14.5^{1}
400	M_3	3.0054	0.0770^{4}	0.0018^{1}	3.5024	$0.0158^{4.5}$	0.0007^{3}	0.9032	$0.0009^{2.5}$	0.0035^{2}	17^{2}
	M_4	3.0073	0.0753^{2}	0.0024^{2}	3.5046	0.0145^{3}	0.0013^{4}	0.9037	$0.0010^{4.5}$	0.0041^{4}	19.5^{4}
	M_5	3.0111	0.0773^{5}	0.0037^{4}	3.5022	$0.0158^{4.5}$	0.0006^{2}	0.9032	$0.0009^{2.5}$	0.0036^{3}	21^{5}

Table 9. Simulation results at $\alpha = 0.4$, $\theta = 0.9$ and $\lambda = 0.2$

		For α			**For θ**			**For λ**			
n	Methods	Average	MSE	RBIAS	Average	MSE	RBIAS	Average	MSE	RBIAS	$\sum$Ranks
	M_1	0.4403	0.3019^{1}	0.1008^{1}	0.8949	0.0266^{1}	0.0057^{1}	0.3599	0.1727^{2}	0.7995^{1}	7^{1}
	M_2	0.5881	0.8862^{5}	0.4703^{5}	0.7954	0.0459^{5}	0.1162^{5}	0.5058	0.2093^{5}	1.5292^{5}	30^{5}
100	M_3	0.5303	0.4705^{3}	0.3256^{4}	0.8128	0.0366^{3}	0.0969^{4}	0.4718	0.1863^{3}	1.3951^{3}	20^{3}
	M_4	0.5218	0.5754^{4}	0.3044^{3}	0.8248	0.0414^{4}	0.0835^{3}	0.4931	0.2067^{4}	1.4652^{4}	22^{4}
	M_5	0.5189	0.4376^{2}	0.2975^{2}	0.8249	0.0311^{2}	0.0833^{2}	0.4315	0.1657^{1}	1.1577^{2}	11^{2}
	M_1	0.4144	0.0401^{1}	0.0359^{1}	0.8735	0.0190^{1}	0.0295^{1}	0.3407	0.1472^{1}	0.7034^{1}	6^{1}
	M_2	0.4599	0.1867^{5}	0.1498^{5}	0.8042	0.0301^{5}	0.1065^{5}	0.4859	0.1928^{5}	1.4296^{5}	30^{5}
200	M_3	0.4425	0.0823^{2}	0.1062^{3}	0.8179	0.0244^{4}	0.0911^{4}	0.4518	0.1763^{3}	1.2589^{3}	19^{3}
	M_4	0.4441	0.1751^{4}	0.1101^{4}	0.8195	0.0271^{3}	0.0895^{3}	0.4719	0.1873^{4}	1.3599^{4}	22^{4}
	M_5	0.4405	0.1153^{3}	0.1013^{2}	0.8221	0.0224^{2}	0.0865^{2}	0.4341	0.1679^{2}	1.1705^{2}	13^{2}
	M_1	0.4323	0.1216^{5}	0.0814^{3}	0.8634	0.0161^{1}	0.0407^{1}	0.3246	0.1385^{1}	0.6229^{1}	$12^{1.5}$
	M_2	0.4373	0.0537^{4}	0.0932^{5}	0.8114	0.0239^{5}	0.0984^{5}	0.4518	0.1679^{5}	1.2589^{5}	29^{5}
300	M_3	0.4368	0.0468^{1}	0.0919^{4}	0.8218	0.0201^{3}	0.0868^{4}	0.4157	0.1544^{3}	1.0786^{3}	18^{3}
	M_4	0.4263	0.0496^{3}	0.0658^{1}	0.8219	0.0223^{4}	0.0867^{3}	0.4429	0.1651^{4}	1.2148^{4}	19^{4}
	M_5	0.4322	0.0469^{2}	0.0804^{2}	0.8288	0.0181^{2}	0.0791^{2}	0.3999	0.1441^{2}	0.9998^{2}	$12^{1.5}$
	M_1	0.4175	0.0209^{1}	0.0438^{4}	0.8596	0.0147^{1}	0.0449^{1}	0.3274	0.1361^{1}	0.6368^{1}	9^{1}
	M_2	0.4185	0.0297^{5}	0.0461^{5}	0.8118	0.0226^{5}	0.0979^{5}	0.4558	0.1739^{5}	1.2792^{5}	30^{5}
400	M_3	0.4163	0.0263^{2}	0.0408^{2}	0.8206	0.0187^{3}	0.0882^{3}	0.4263	0.1583^{3}	1.1317^{3}	16^{3}
	M_4	0.4119	0.0278^{4}	0.0297^{1}	0.8203	0.0211^{4}	0.0885^{4}	0.4451	0.1689^{4}	1.2254^{4}	21^{4}
	M_5	0.4174	0.0274^{3}	0.0436^{3}	0.8248	0.0174^{2}	0.0836^{2}	0.4111	0.1526^{2}	1.0553^{2}	14^{2}

$$\ell = \log L = n\log\alpha + n\log\theta + n\log(1+\alpha) + \theta\sum_{i=1}^{n} w_i - 2\sum_{i=1}^{n}\log\left(1+\alpha e^{\theta w_i}\right) + \sum_{i=1}^{n}\log\left(1-\lambda+\frac{2\lambda(1+\alpha)}{1+\alpha e^{\theta w_i}}\right).$$

The MLEs of the parameters α, θ and λ, are derived by maximizing the function ℓ. We can verify this by calculating the first derivatives of the function ℓ and equating the outcomes to zero, which will provide the estimates of the TP

Table 10. Partial and total rankings of all estimating techniques for the TP distribution

Parameters	n	$\mathbf{M_1}$	$\mathbf{M_2}$	$\mathbf{M_3}$	$\mathbf{M_4}$	$\mathbf{M_5}$
α=1.2, θ=2, λ=0.6	100	4	3	2	5	1
	200	3.5	2	3.5	1	5
	300	1	5	2	4	3
	400	1	5	2	3.5	3.5
α=1.4, θ=1.8, λ=0.5	100	4.5	3	4.5	1	2
	200	3	4	1.5	5	1.5
	300	3	4	2	5	1
	400	3	5	1	4	2
α=1.5, θ=2.5, λ=0.8	100	3	5	4	1	2
	200	3	1	4	2	5
	300	3	5	1.5	4	1.5
	400	5	3.5	1	3.5	2
α=2, θ =2.8, λ=0.6	100	4	5	2	3	1
	200	1	5	4	3	2
	300	1.5	3	1.5	5	4
	400	1	2	3	4.5	4.5
α=2.5, θ =3, λ=0.7	100	2	1	3	4	5
	200	1	3	5	2	4
	300	2	3.5	1	5	3.5
	400	2	3	4.5	1	4.5
α=3, θ =3.5, λ=0.9	100	2.5	4	1	5	2.5
	200	3.5	3.5	2	1	5
	300	3.5	1.5	5	1.5	3.5
	400	3	1	2	4	5
α=0.4, θ =0.9, λ=0.2	100	1	5	3	4	2
	200	1	5	3	4	2
	300	1.5	5	3	4	1.5
	400	1	5	3	4	2
$\sum$**Ranks overall ranks**		68.5	101	75	94	81.5
		1	5	2	4	3

distribution as below:

$$\frac{\partial \ell}{\partial \alpha} = \frac{n}{\alpha} + \frac{n}{1+\alpha} - 2\sum_{i=1}^{n} \frac{e^{\theta w_i}}{1+\alpha e^{\theta w_i}} + \sum_{i=1}^{n} \frac{2\lambda\left(1-e^{\theta w_i}\right)}{\left[2\lambda(1+\alpha)+\left(1+\alpha e^{\theta w_i}\right)(1-\lambda)\right]\left(1+\alpha e^{\theta w_i}\right)}, \tag{14}$$

$$\frac{\partial \ell}{\partial \theta} = \frac{n}{\theta} + \sum_{i=1}^{n} w_i - 2\sum_{i=1}^{n} \frac{\alpha w_i e^{\theta w_i}}{1+\alpha e^{\theta w_i}} - \sum_{i=1}^{n} \frac{2\lambda\alpha w_i(1+\alpha)\left(1+\alpha e^{\theta w_i}\right)^{-2}}{1-\lambda+\frac{2\lambda(1+\alpha)}{1+\alpha e^{\theta w_i}}}, \tag{15}$$

$$\frac{\partial \ell}{\partial \lambda} = \sum_{i=1}^{n} \frac{-1+\frac{2(1+\alpha)}{1+\alpha e^{\theta w_i}}}{1-\lambda+\frac{2\lambda(1+\alpha)}{1+\alpha e^{\theta w_i}}} = \sum_{i=1}^{n} \frac{1+2\alpha-\alpha e^{\theta w_i}}{1-\lambda+2\lambda(1+\alpha)+\alpha e^{\theta w_i}(1-\lambda)}. \tag{16}$$

By setting the Eqs. (14), (15) and (16) to zero, we can obtain the estimates of the parameters α, θ and λ, respectively. Under standard regularity conditions for lifetime distributions, the TP log-likelihood is continuous and bounded and tends to $-\infty$ at the parameter boundaries, so the score equations (14)–(16) admit a solution. Uniqueness can be verified numerically from the monotonicity of the score functions. The resulting MLEs are consistent and asymptotically normal under these conditions. The non-classical estimators (MPS, LS, WLS, CM, AD) inherit their asymptotic properties from the standard theory established in the literature. A full proof is not provided because the paper focuses on model construction and applied comparison, but the theoretical basis is now explicit.

6.2. Bayesian estimation

Bayesian estimation offers a stable and adaptable framework that combines empirical data with prior knowledge to infer unknown parameters. In this study, we suggest Gamma prior distributions for the parameters α, θ, and a proper uniform prior on $[-1,1]$ to the transmutation parameter λ, and the joint prior density function is given by:

$$\pi(\alpha)=\alpha^{a_1-1}e^{-b_1\alpha},\ \alpha>0,\qquad \pi(\theta)=\theta^{a_2-1}e^{-b_2\theta},\ \theta>0,\qquad \pi(\lambda)=\frac{1}{2},\ -1\le\lambda\le 1,$$

where a_i and b_i, for $i=1,2,3$, are the hyperparameters which is supposed to represent the prior distribution of the unknown parameter. The independent Gamma priors are chosen due to the flexibility of this distribution. By means of Bayes' theorem, the posterior density of α, θ and λ is calculated as the product of the likelihood function and the prior distribution and is given by:

$$\pi^*(\alpha,\theta,\lambda\,|\,w)=\frac{\pi(\alpha)\pi(\theta)\pi(\lambda)L(\alpha,\theta,\lambda\,|\,w)}{\int_0^\infty\int_0^\infty\int_{-1}^1\pi(\alpha)\pi(\theta)\pi(\lambda)L(\alpha,\theta,\lambda\,|\,w)\,d\alpha\,d\theta\,d\lambda}. \tag{17}$$

It is vital for the practical purpose of Bayesian inference to consider both symmetric and asymmetric loss functions. A loss function is basically a numerical measure of how far our candidate parameter values are from their correct estimates. The symmetric type is well known to most folks, in particular squared error loss (SEL) according to [34]. But asymmetric loss functions give us far more freedom especially when we are in a situation where overestimating a value is more costly than underestimating it. That flexibility is precisely what makes Bayesian estimators dependable and robust, and able to do well in many practical scenarios. The formula for SEL function is:

$$L(\eta-\widehat{\eta})=(\eta-\widehat{\eta})^2,$$

where $\eta=(\alpha,\theta,\lambda)$.

Consequently, the Bayesian estimate of a function $g(\alpha,\theta,\lambda)$ under the SEL criterion, is represented by the posterior mean:

$$\widehat{g}_{BS}(\alpha,\theta,\lambda\,|\,w)=E_{\alpha,\theta,\lambda|w}\left(g(\alpha,\theta,\lambda)\right)$$

and

$$E_{\alpha,\theta,\lambda}\left(g(\alpha,\theta,\lambda)\right)=\frac{\int_0^\infty\int_0^\infty\int_{-1}^1 g(\alpha,\theta,\lambda)\pi(\alpha)\pi(\theta)\pi(\lambda)L(\alpha,\theta,\lambda\,|\,w)\,d\alpha\,d\theta\,d\lambda}{\int_0^\infty\int_0^\infty\int_{-1}^1\pi(\alpha)\pi(\theta)\pi(\lambda)L(\alpha,\theta,\lambda\,|\,w)\,d\alpha\,d\theta\,d\lambda}. \tag{18}$$

It is significant to note that the proportion of various integrals in Eq. (18) cannot be explicitly defined. The MCMC technique is utilized to generate samples from the joint posterior density function as indicated in Eq. (17). The MCMC methodology is particularly executed thru the Gibbs sampling within the Metropolis-Hastings (M-H) framework; see also [46, 48, 49] for similar MCMC-based Bayesian inference in lifetime models. The subsequent representation is the aggregated posterior distribution:

$$\pi_1^*(\alpha\,|\,\theta,\lambda)\propto\pi(\alpha)\alpha^n\prod_{i=1}^n\frac{(1+\alpha)}{(1+\alpha e^{\theta w_i})^2}\left[1-\lambda+\frac{2\lambda(1+\alpha)}{1+\alpha e^{\theta w_i}}\right], \tag{19}$$

$$\pi_2^*(\theta\,|\,\alpha,\lambda)\propto\pi(\theta)\theta^n\prod_{i=1}^n e^{\theta w_i}\frac{1}{(1+\alpha e^{\theta w_i})^2}\left[1-\lambda+\frac{2\lambda(1+\alpha)}{1+\alpha e^{\theta w_i}}\right], \tag{20}$$

and

$$\pi_3^*(\lambda\,|\,\alpha,\theta)\propto\pi(\lambda)\prod_{i=1}^n\left[1-\lambda+\frac{2\lambda(1+\alpha)}{1+\alpha e^{\theta w_i}}\right]. \tag{21}$$

In the Metropolis–Hastings step for λ, candidate values are drawn from a truncated normal proposal on $[-1,1]$ and rejected if they fall outside this interval. Due to the structural complexity of the TP distribution, there are no closed-form Bayesian estimates of α, θ and λ. To circumvent this processing constraint, the authors suggest

to apply MCMC methods, a reliable alternative for posterior approximation in analytically intractable scenarios. From Equations (19) and (20), it can be seen that the conditional posterior densities of these parameters do not follow any standard distributions, so the Gibbs sampling along with the Metropolis–Hastings algorithm is required to help generate samples. The generated MCMC algorithm runs a Markov chain whose stationary distribution is the target posterior, so it gives a sample-based approximation from which summary statistics, mainly the posterior mean, are computed and used as final Bayesian estimates of the three model parameters.

This research conducted an extensive comparison of MLE and Bayesian estimation methods to evaluate the efficacy and adaptability of the suggested distribution. The MLE technique, recognized for its asymptotic efficacy and computational ease, yields point estimates derived exclusively from observable data. Conversely, Bayesian estimation integrates prior convictions and produces comprehensive posterior distributions, providing a more useful framework, especially when faced with few or confused data.

It is useful to compare them to show the respective advantages and practical consequences of each estimation method. MLE can work well for large samples, however Bayesian approaches can provide better inference in the presence of complex models or prior knowledge limitations. In Tables 11–14 a detailed analysis of the point estimates, confidence intervals and numerical results obtained by the two estimation processes is shown, providing a more complete picture of the overall performance of the model. The results show that the MLE outperforms the Bayesian approach, particularly in the estimate precision and the sensitivity to the changes in the sample size. More specifically, the MLE provides parameter estimates with much smaller MSEs and its accuracy improves remarkably with the increase of the sample size. This empirical trend is consistent with the well-known asymptotic features of the MLE.

The comparison results show that MLE has practical advantages in the examined scenarios, which means it is suitable for applications with large datasets where the reduction of estimation error is important. However, Bayesian estimate is still useful in situations of having prior knowledge or dealing with complicated hierarchical models. For the Bayesian analysis, MCMC approaches were used to generate posterior samples. We examined the histograms of these posterior samples to ensure convergence and to get a sense of the shape of the posterior distributions (see Figure 4).

Table 11. Simulation results for $\alpha = 0.5$, $\theta = 1.2$, $\lambda = 0.7$

n	Est	MLE			Bayesian		
		α	θ	λ	α	θ	λ
100	Average	0.2179	1.5591	0.9695	0.6725	1.9821	-0.0729
	RBIAS	0.5641	0.2992	0.3851	0.3449	0.6518	1.1041
	MSE	0.0859	0.1957	0.0984	0.3307	0.6659	0.6521
200	Average	0.2114	1.5283	0.9902	0.6168	2.0320	-0.1218
	RBIAS	0.5772	0.2736	0.4145	0.2336	0.6933	1.1740
	MSE	0.0865	0.1366	0.0922	0.2580	0.7221	0.7481
300	Average	0.2203	1.5206	0.9941	0.6277	2.0615	-0.1675
	RBIAS	0.5594	0.2672	0.4201	0.2554	0.7179	1.2394
	MSE	0.1253	0.1159	0.0962	0.2650	0.7610	0.8323
400	Average	0.2101	1.5112	0.9999	0.6969	2.0399	-0.1938
	RBIAS	0.5798	0.2593	0.4286	0.3939	0.6999	1.2768
	MSE	0.0854	0.1054	0.0899	0.4008	0.7224	0.9089

7. Data Analysis

In this section, we offer two examples of real-world data of different fields, and dependability to highlight the versatility of the TP model. The MLE technique is employed to ascertain the parameters of each model, while R statistical software is utilized for computations. We evaluate the fitting performance of the TP model against various competing models, specifically: the Perk (PE) [22], inverse power Perk (IPP) [26], inverse power Ailamujia (IPA) [35], generalized inverted exponential (GIEx) [36], and inverse exponential (IE) [37] distributions.

Table 12. Simulation results for $\alpha = 0.7$, $\theta = 0.9$, $\lambda = 0.8$

n	Est	MLE			Bayesian		
		α	θ	λ	α	θ	λ
100	Average	0.2875	1.2759	0.9792	0.7775	1.6696	-0.0359
	RBIAS	0.5893	0.4178	0.2241	0.1107	0.8551	1.0449
	MSE	0.1974	0.1883	0.0531	0.4598	0.6304	0.7477
200	Average	0.2689	1.2578	0.9959	0.7392	1.7103	-0.1058
	RBIAS	0.6159	0.3975	0.2449	0.0561	0.9004	1.1323
	MSE	0.1952	0.1466	0.0423	0.3198	0.6742	0.8876
300	Average	0.2789	1.2403	0.9961	0.7042	1.7189	-0.1069
	RBIAS	0.6016	0.3781	0.2451	0.0059	0.9099	1.1337
	MSE	0.1881	0.1312	0.0419	0.2888	0.6843	0.8954
400	Average	0.2746	1.2358	0.9999	0.7621	1.7226	-0.1665
	RBIAS	0.6077	0.3731	0.2499	0.0886	0.9139	1.2081
	MSE	0.1901	0.1223	0.0399	0.3156	0.6859	1.0155

Table 13. Simulation results for $\alpha = 1.2$, $\theta = 1$, $\lambda = 0.8$

n	Est	MLE			Bayesian		
		α	θ	λ	α	θ	λ
100	Average	0.4959	1.4241	0.9702	1.0554	1.9203	0.0353
	RBIAS	0.5867	0.4241	0.2127	0.1204	0.9203	0.9559
	MSE	0.5881	0.2944	0.0559	0.5927	0.9052	0.6315
200	Average	0.5012	1.3733	0.9959	0.9734	2.0113	-0.0584
	RBIAS	0.5823	0.3733	0.2448	0.1889	1.0113	1.0731
	MSE	0.5781	0.1989	0.0413	0.4528	1.0522	0.8009
300	Average	0.5368	1.3436	0.9903	0.9904	2.0291	-0.0856
	RBIAS	0.5526	0.3436	0.2379	0.1747	1.0291	1.1070
	MSE	0.5593	0.1750	0.0489	0.5254	1.0787	0.8544
400	Average	0.5117	1.3496	0.9970	1.0092	2.0499	-0.1221
	RBIAS	0.5736	0.3496	0.2463	0.1589	1.0499	1.1526
	MSE	0.5641	0.1687	0.0407	0.4875	1.1175	0.9216

Table 14. Simulation results for $\alpha = 0.2$, $\theta = 0.7$, $\lambda = 0.6$

n	Est	MLE			Bayesian		
		α	θ	λ	α	θ	λ
100	Average	0.1358	0.9639	0.4865	0.2314	1.0412	-0.0642
	RBIAS	0.3211	0.3769	0.1892	0.1572	0.4999	1.1070
	MSE	0.0299	0.0997	0.3627	0.0552	0.1354	0.4988
200	Average	0.1144	0.9426	0.5461	0.2139	1.0449	-0.0902
	RBIAS	0.4282	0.3466	0.0899	0.0693	0.4929	0.9457
	MSE	0.0128	0.0817	0.2778	0.0262	0.1247	0.5442
300	Average	0.1071	0.9364	0.5834	0.2179	1.0447	-0.0954
	RBIAS	0.4642	0.3378	0.0277	0.0899	0.4923	0.9543
	MSE	0.0115	0.0789	0.2508	0.0334	0.1233	0.5752
400	Average	0.1103	0.9358	0.5723	0.2405	1.0438	-0.1277
	RBIAS	0.4486	0.3369	0.0461	0.2023	0.4783	0.9647
	MSE	0.0148	0.0774	0.2562	0.0378	0.1171	0.6632

Utilizing the classical methodology, we have employed various model selection criteria and goodness-of-fit statistics. For model selection, we employed Akaike information criterion (A_1), Bayesian information criterion (A_2), corrected Akaike information criterion (A_3), Hannan-Quinn information criterion (A_4). For the goodness-of-fit assessment, we utilized the Kolmogorov-Smirnov (A_5) test statistic, along with related p-value (A_6). The efficacy of the parameter estimator for the TP model across the two datasets was evaluated employing ML, MPS, and LSE methodologies, utilizing the Kolmogorov-Smirnov (A_5) test statistic, along with related p-value (A_6). We

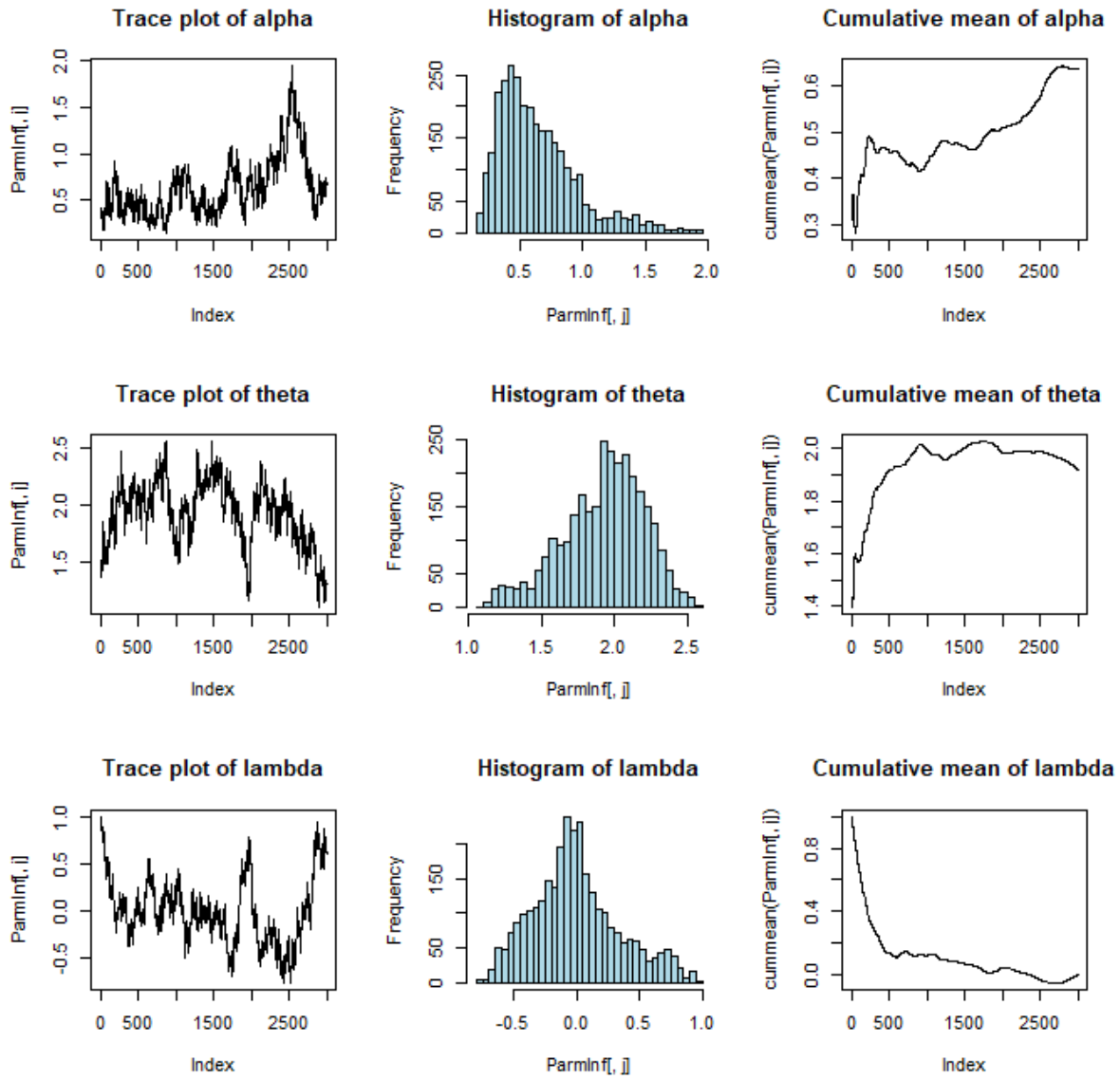


Figure 4. Plots of trace, histogram, and cumulative mean at $\alpha = 0.5$, $\theta = 1.2$, $\lambda = 0.7$.

derived the estimators of the new model for the utilized techniques pertaining to the datasets under consideration. We have demonstrated the application of the TP with the classical methodology as outlined below.

7.1. Data set I

The initial set of data is analyzed by Murthy et al. [38], and it reflects the time between failures for a repairable item. The data values are: 1.43, 0.11, 0.71, 0.77, 2.63, 1.49, 3.46, 2.46, 0.59, 0.74, 1.23, 0.94, 4.36, 0.40, 1.74, 4.73, 2.23, 0.45, 0.70, 1.06, 1.46, 0.30, 1.82, 2.37, 0.63, 1.23, 1.24, 1.97, 1.86, 1.17. Figure 5 illustrates the initial PDF formulas for the dataset with the non-parametric kernel density estimation method. The PDF of the dataset exhibits asymmetry. Furthermore, Figure 5 employs the quantile–quantile (QQ) plot to evaluate the normality criterion. The

boxplot shows that the data is right-skewed with presence of outliers. It is clear from the TTT plot that the data has an increasing HRF. Also, the data is analyzed with some descriptive measures in Table 15.

Table 16 presents the MLEs of the parameters for each distribution, along with the goodness of fit metrics A_1, A_2, A_3, A_4, A_5 and A_6 for each distribution. We determine that the TP distribution provides the optimal fit due to its minimal values of A_1, A_2, A_3, A_4, A_5 with the maximal value of A_6. Consequently, one may ascertain that the TP distribution surpasses the other distributions for the analyzed dataset. Figure 6 illustrates the estimated PDF, empirical CDF, and P-P plots of the competing distributions, demonstrating that our distribution aligns closely with the dataset presented. Table 17 presents the estimated values for several estimating methods of the TP model across this dataset, demonstrating that the CME method surpasses the others in all datasets, as indicated by the greatest A_6. Additionally, a graphic relationship of the nature of this dataset with the fitted PDFs, CDFs, and P-P plots over all estimation methods are presented in Figures 7–9.

Table 15. Descriptive measures for dataset I

Dataset	n	Mean	Median	Variance	Skewness	Kurtosis	Range	Min	Max
I	30	1.542	1.235	1.271	1.295	4.319	4.62	0.11	4.73

Table 16. Some goodness of fit measures for dataset I

Models	MLEs	A_1	A_2	A_3	A_4	A_5	A_6
TP	$\widehat{\alpha}=0.2150$ $\widehat{\theta}=1.1899$ $\widehat{\lambda}=0.3994$	86.814	91.018	87.737	88.159	0.071	0.998
PE	$\widehat{\alpha}=7.7277$ $\widehat{\beta}=0.1189$	96.027	98.829	96.471	96.923	0.189	0.232
IPP	$\widehat{\alpha}=3776.1$ $\widehat{\beta}=1.0734$ $\widehat{\lambda}=0.7519$	98.751	102.955	99.674	100.096	0.134	0.656
IPA	$\widehat{\alpha}=1.7979$ $\widehat{\beta}=0.7858$	92.701	95.503	93.145	93.597	0.128	0.706
GIEx	$\widehat{\alpha}=1.6684$ $\widehat{\lambda}=1.0976$	93.931	96.734	94.376	94.828	0.163	0.401
IE	$\widehat{\lambda}=0.7934$	95.066	96.467	95.209	95.514	0.160	0.423

Table 17. Comparison between estimation methods for dataset I

Methods	Estimates of parameters			Measures of adequacy	
	α	θ	λ	A_5	A_6
MLE	0.2150	1.1899	0.3994	0.0709	0.9982
MPS	0.1715	1.3304	0.3423	0.0716	0.9979
LSE	0.2063	1.2359	0.3809	0.0717	0.9978
WLSE	0.2013	1.2010	0.4351	0.0702	0.9985
CME	0.1715	1.3677	0.3184	0.0650	0.9996
ADE	0.1885	1.2173	0.4594	0.0709	0.9982

7.2. Data set II

This second dataset consists of a subset that was taken from Tahani's findings [39]. It indicates the duration of survival, quantified in years, for a cohort of patients undergoing chemotherapy. The dataset contains 46 survival durations, each linked to a unique patient. The values are: 0.047, 0.115, 0.121, 0.132, 0.164, 0.197, 0.203, 0.260, 0.282, 0.296, 0.334, 0.395, 0.458, 0.466, 0.501, 0.507, 0.529, 0.534, 0.540, 0.570, 0.641, 0.644, 0.696, 0.841, 0.863, 1.099, 1.219, 1.271, 1.326, 1.447, 1.485, 1.553, 1.581, 1.589, 2.178, 2.343, 2.416, 2.444, 2.825, 2.830, 3.578, 3.658,

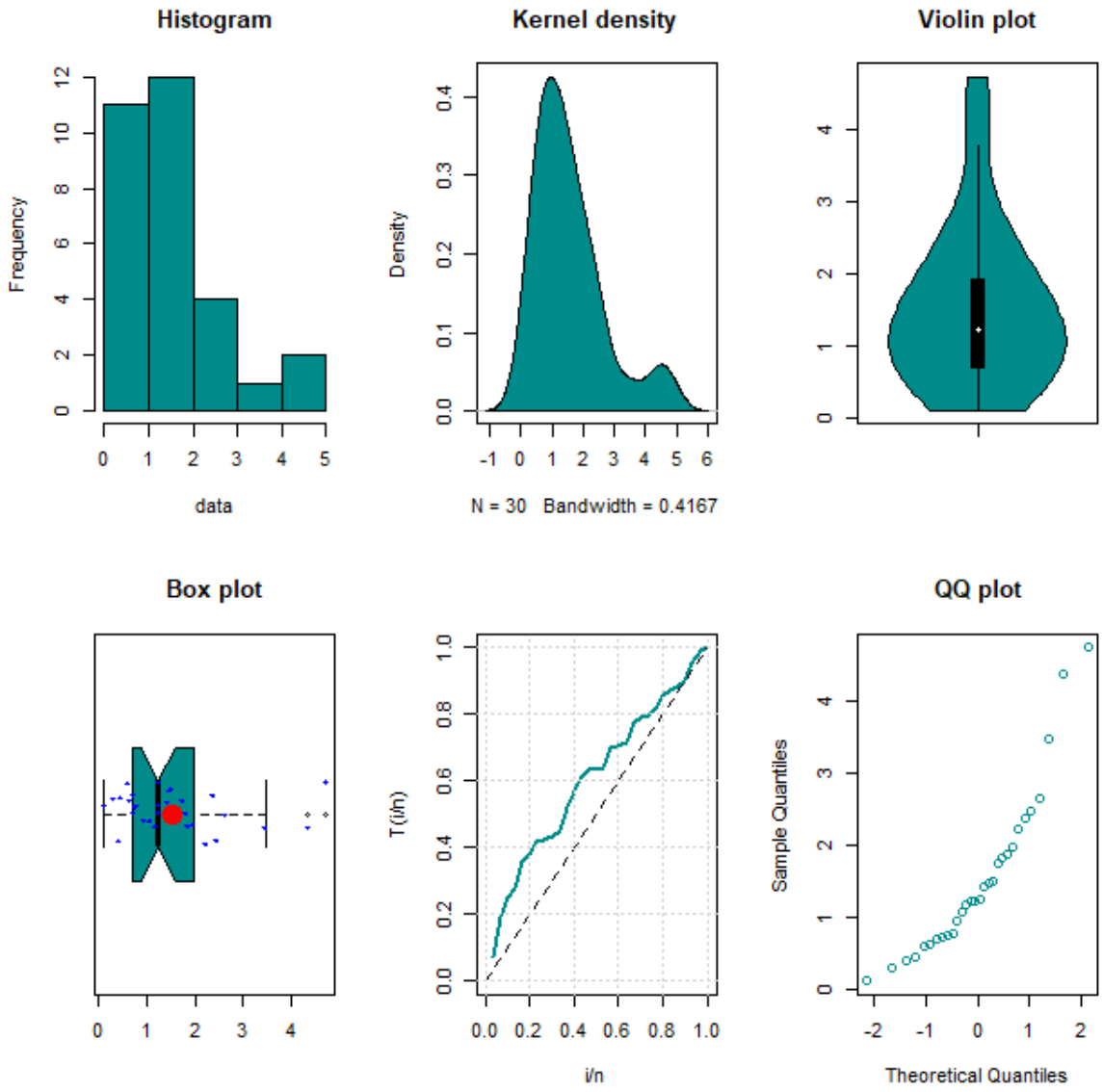


Figure 5. Some non-parametric plots for the first dataset.

3.743, 3.978, 4.003, 4.033. Table 18 displays some descriptive measures of the data. Figure 10 illustrates the TTT-plot, Q-Q plot, box plot, histogram, and kernel density estimation of the examined dataset. This illustration clearly indicates that the data exhibits a rightward skew and an escalating failure rate.

Employing the MLE method for parameter estimation and goodness-of-fit assessment, Table 19 display the results for parameter estimations. The analysis underscores that among all competing models, the TP model exhibits superior performance, as indicated by its minimal values across several goodness-of-fit metrics such as A_1, A_2, A_3, A_4, A_5 statistics, and significant A_6. Additionally, the graphical plots in Figure 11 supports the results in Table 19. The comparative analysis of parameter estimate methods for the TP model for the second dataset is summarized in Table 20, which clearly shows the superiority of the CME method that obtains the highest A_6 measure in all the studied datasets. To further understand the data structure, the authors provide graphical results

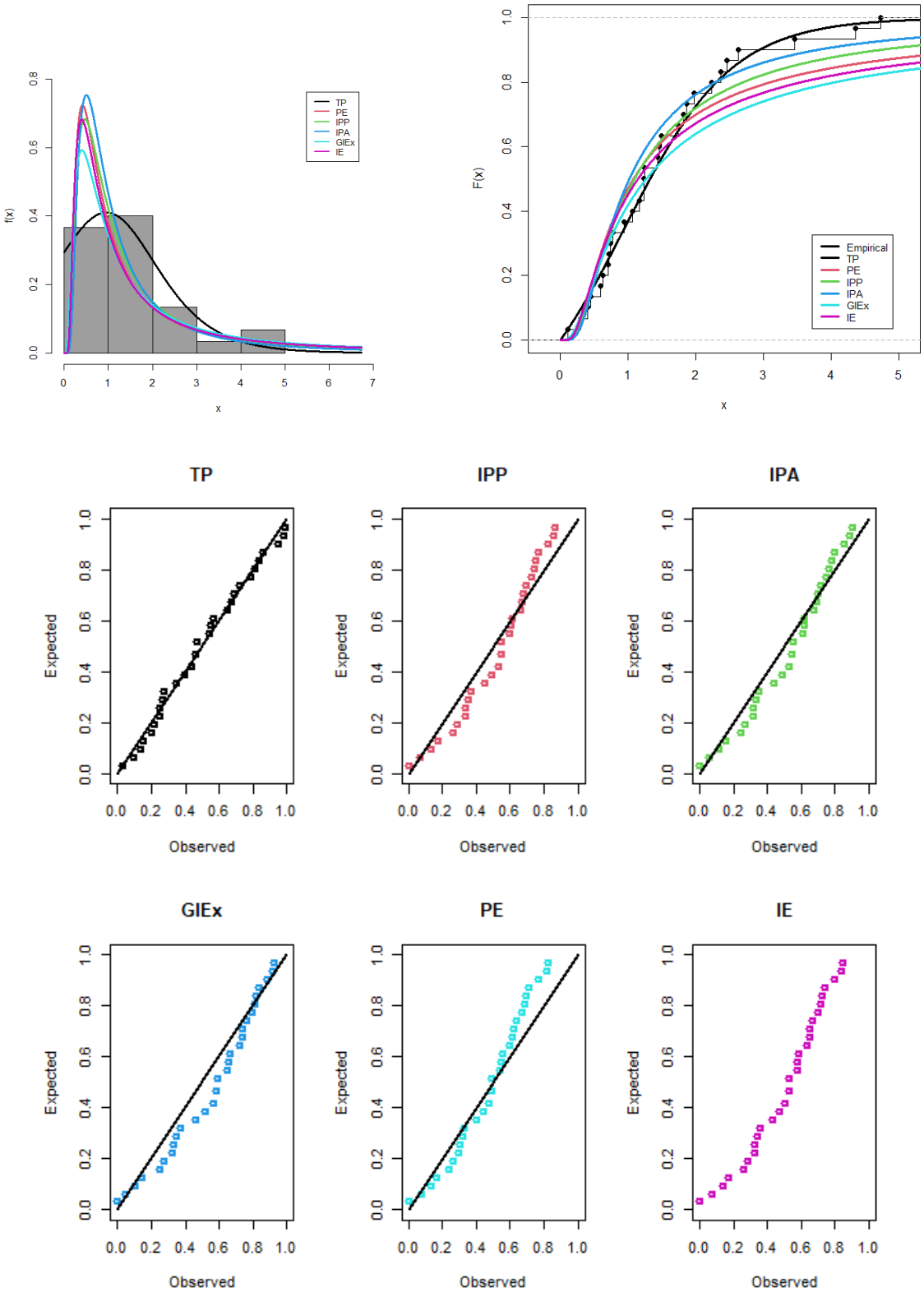


Figure 6. Graphs of estimated PDF, empirical CDF and P-P plots for dataset 1.

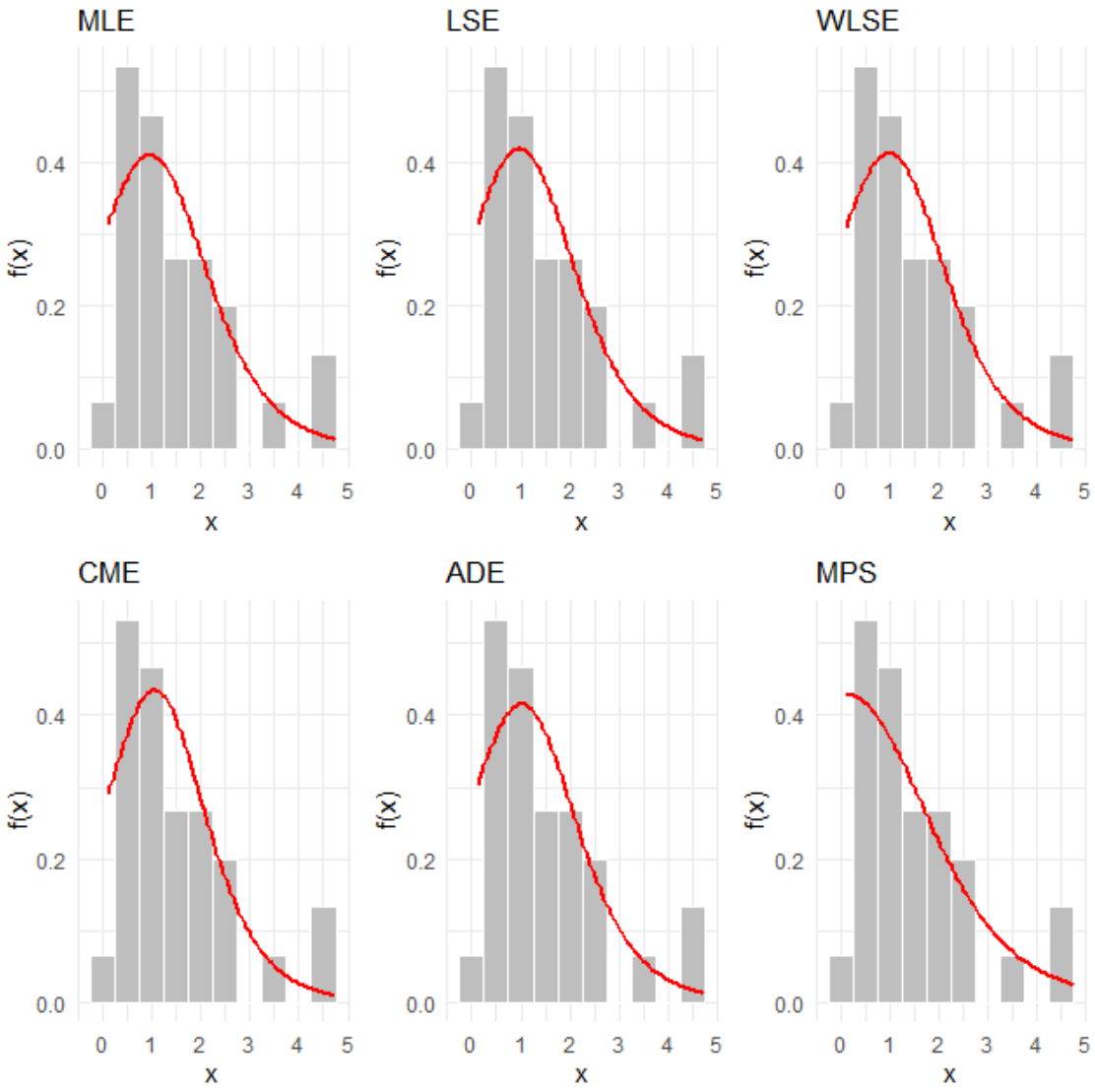


Figure 7. Graphical comparison of estimated PDF for dataset I.

in Figures 12–14, showing the fitted PDFs, CDFs and P–P plots for each estimating method, thereby providing numerical and visual validation of the advantage of the CME.

Table 18. Descriptive measures for dataset II

Dataset	n	Mean	Median	Variance	Skewness	Kurtosis	Range	Min	Max
II	46	1.325	0.7685	1.532	1.0061	2.7347	3.986	0.047	4.033

A critical observation from Tables 16 and 19 is the direct performance gap between the TP distribution and other Perk-based models (PE and IPP). Specifically, the addition of the transmutation parameter λ significantly reduces information loss metrics (AIC, BIC, CAIC, and HQIC) and achieves lower Kolmogorov-Smirnov test statistics with markedly higher p-values compared to both the baseline Perk and its inverse power variant. This confirms

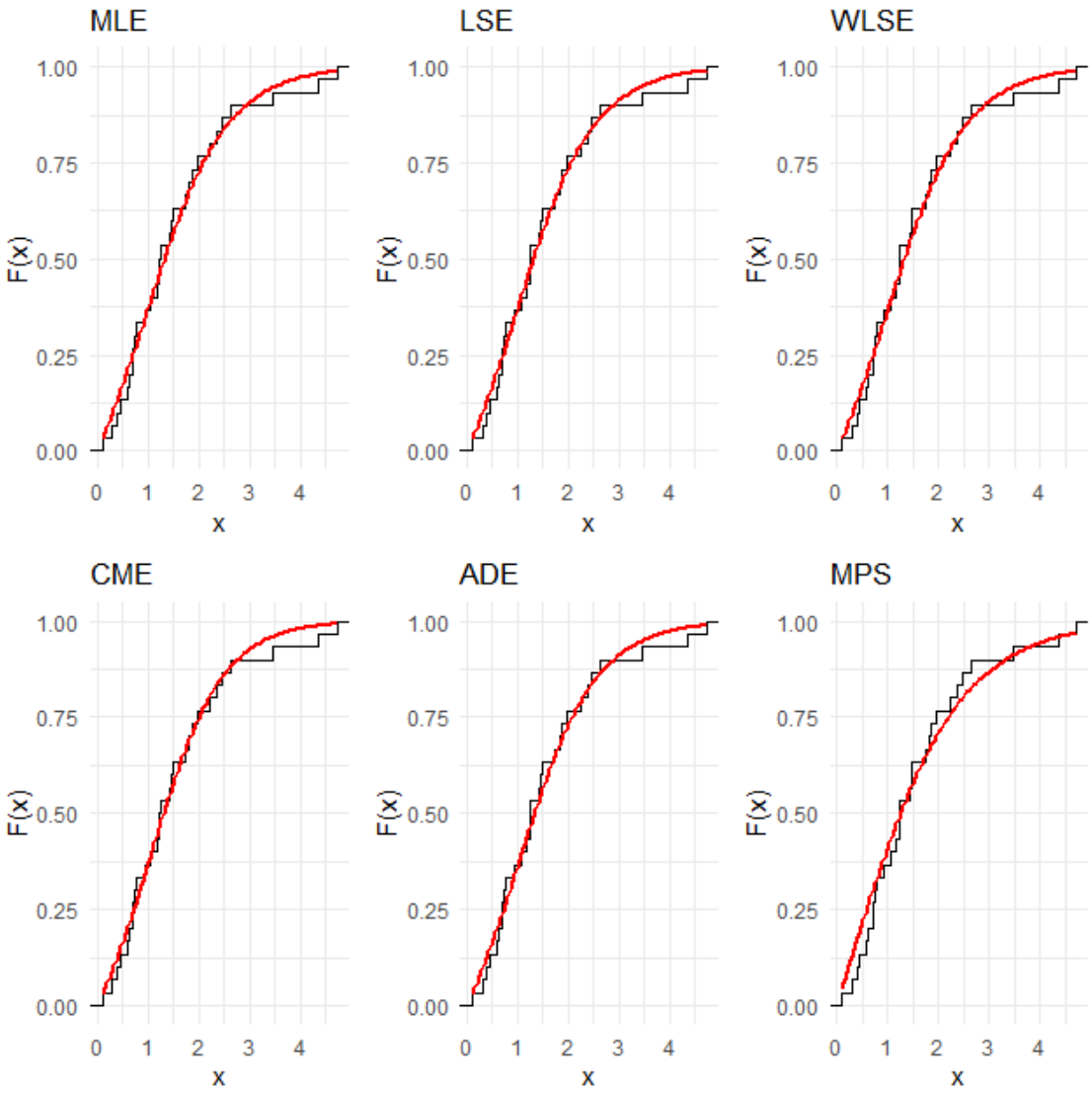


Figure 8. Graphical comparison of estimated CDF for dataset I.

that the TP model provides a demonstrably superior mathematical representation for lifetime datasets displaying skewness and non-monotonic failure rates.

The practical implementations on Dataset I and Dataset II offer distinct domain-specific insights that justify the model's adoption:

- Reliability Engineering Insight: For repairable industrial devices (Dataset I), failure intervals are heavily influenced by cumulative stress. The TP model's ability to fit increasing hazard rates with minimal information loss (AIC = 86.814, p-value = 0.998) provides reliability engineers with a highly reliable tool for scheduling preventive maintenance before system wear-out occurs.
- Biomedical Survival Insight: In clinical oncology (Dataset II), patient survival post-chemotherapy often exhibits high initial mortality risk followed by a prolonged survival tail. The TP distribution accurately models this acute risk phase via its transmuted structure ($\lambda = 0.0082$), providing oncologists with more

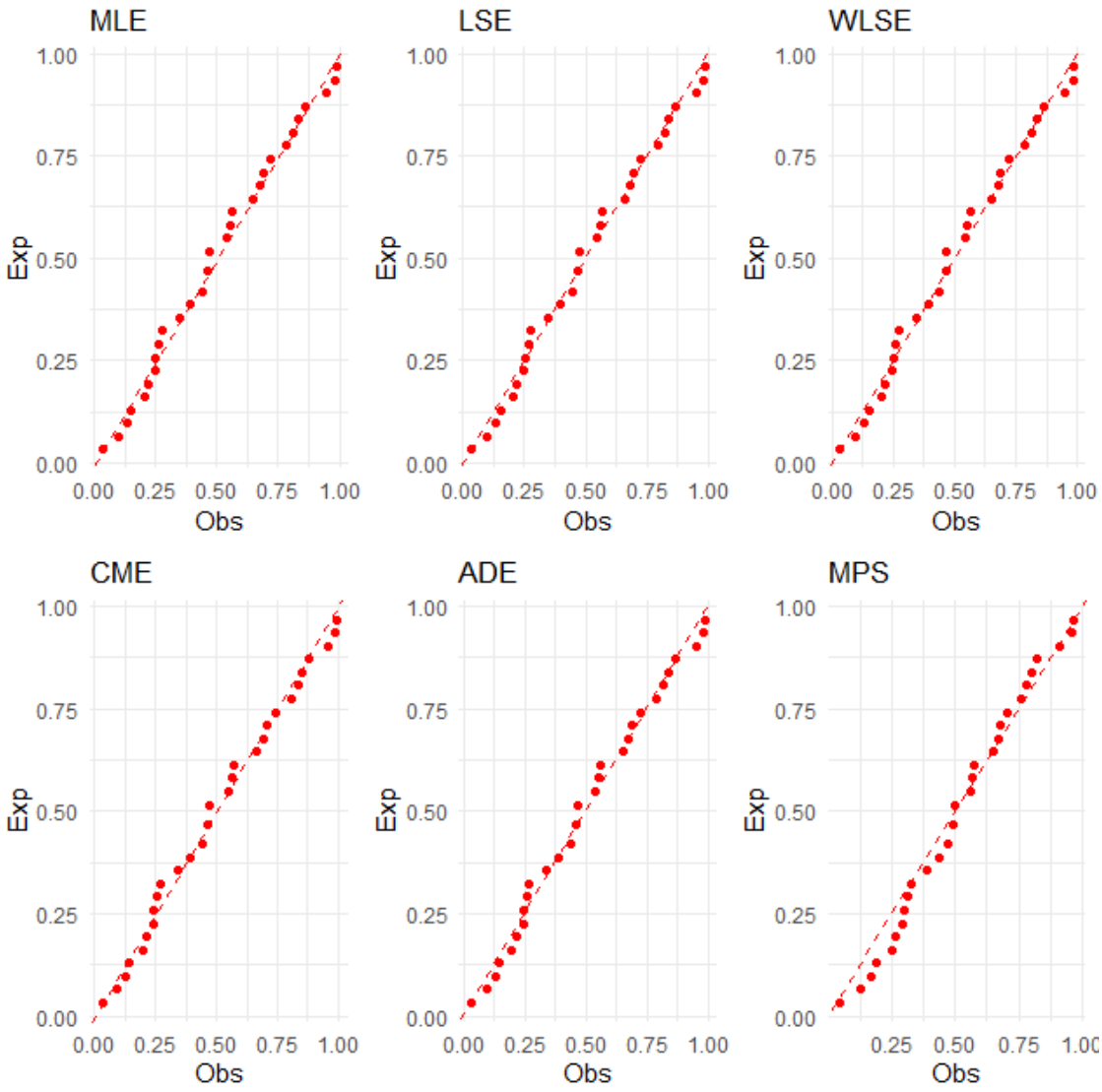


Figure 9. Graphical comparison of P-P plots for dataset I.

precise quantile survival estimates (Q_1, Q_2, Q_3) for patient prognosis compared to traditional single-parameter or un-transmuted models.

7.3. Unique Statistical and Applied Advantages of the TP Model

Based on theoretical derivations, simulation results, and real-data applications, the Transmuted Perk (TP) distribution demonstrates three unique advantages over classical and existing Perk-type distributions:

- Enhanced Tail Behavior and Skewness Adaptability: The inclusion of the transmutation parameter λ enables the model to accommodate heavy-tailed behavior and varying degrees of right-skewness without requiring additional shape parameters. In Dataset I and Dataset II, which exhibit right-skewed empirical distributions with heavy tails (kurtosis values of 4.319 and 2.7347, respectively), the TP distribution superiorly fitted the tail behavior, yielding the lowest information loss metrics (AIC = 86.814 and 123.867).

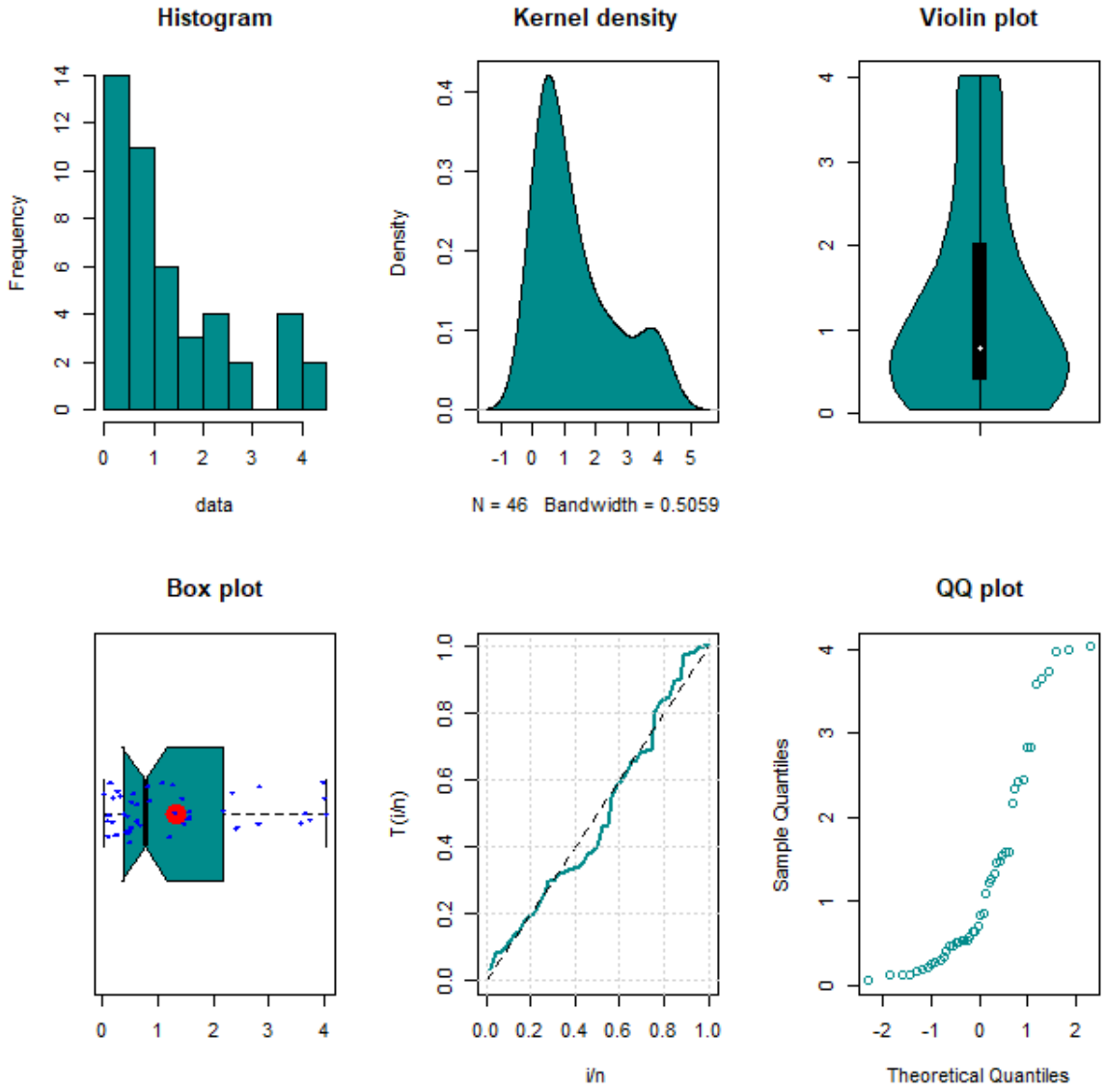


Figure 10. Some non-parametric plots for dataset II.

- Superior Risk-Rate (HRF) Modeling: Unlike baseline Perk or Inverse Power Perk models that have limited failure rate shapes, the TP distribution accommodates non-monotonic hazard rate functions, particularly unimodal (upside-down bathtub) curves alongside increasing and decreasing profiles (Figure 1). This provides superior risk modeling for biomedical survival data (Dataset II), where patient mortality risk peaks shortly post-treatment before stabilizing over time.
- Robust and Reliable Finite-Sample Inference: The systematic comparison of seven estimation procedures proves that non-classical frequentist estimators, specifically Cramér-von Mises Estimation (CME) and Maximum Product of Spacings (MPS), provide highly robust parameter estimates even under moderate sample sizes. In empirical fitting, CME yielded outstanding goodness-of-fit adequacy (p-value = 0.9996

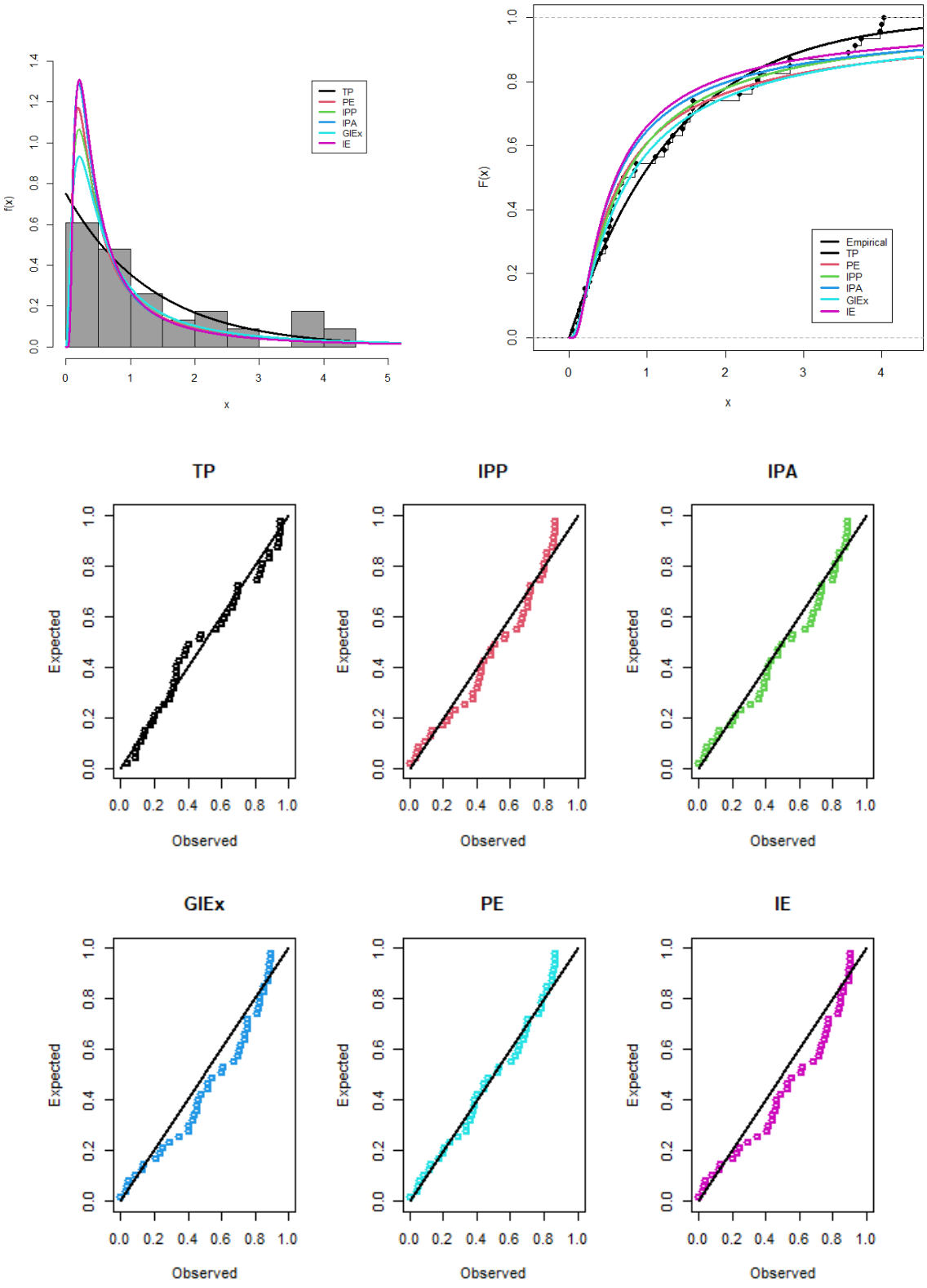


Figure 11. Graphs of estimated PDF, empirical CDF and P-P plots for dataset II.

Table 19. Some goodness of fit measures for dataset II

Models	MLEs	A_1	A_2	A_3	A_4	A_5	A_6
TP	$\widehat{\alpha} = 77.425$ $\widehat{\theta} = 0.7596$ $\widehat{\lambda} = 0.0082$	123.867	129.353	124.438	125.922	0.094	0.772
PE	$\widehat{\alpha} = 3.1898$ $\widehat{\beta} = 0.1882$	129.035	132.692	129.314	130.405	0.135	0.337
IPP	$\widehat{\alpha} = 5518.6$ $\widehat{\beta} = 0.8756$ $\widehat{\lambda} = 0.4948$	134.830	140.316	135.402	136.885	0.136	0.334
IPA	$\widehat{\alpha} = 1.3533$ $\widehat{\beta} = 0.6172$	128.963	132.620	129.242	130.332	0.113	0.563
GIEx	$\widehat{\alpha} = 0.9228$ $\widehat{\lambda} = 0.3912$	134.376	138.033	134.655	135.746	0.140	0.302
IE	$\widehat{\lambda} = 0.4133$	132.546	134.374	132.636	133.231	0.147	0.246

Table 20. Comparison between estimation methods for dataset II

Methods	**Estimates of parameters**			**Measures of adequacy**	
	α	θ	λ	A_5	A_6
MLE	77.425	0.7596	0.0082	0.094	0.7715
MPS	10.262	0.7997	0.0024	0.097	0.7394
LSE	7812.3	0.5513	0.4673	0.081	0.8956
WLSE	7281.2	0.6330	0.2593	0.086	0.8593
CME	3172.5	0.5562	0.4593	0.081	0.9032
ADE	2719.5	0.5904	0.3536	0.086	0.8612

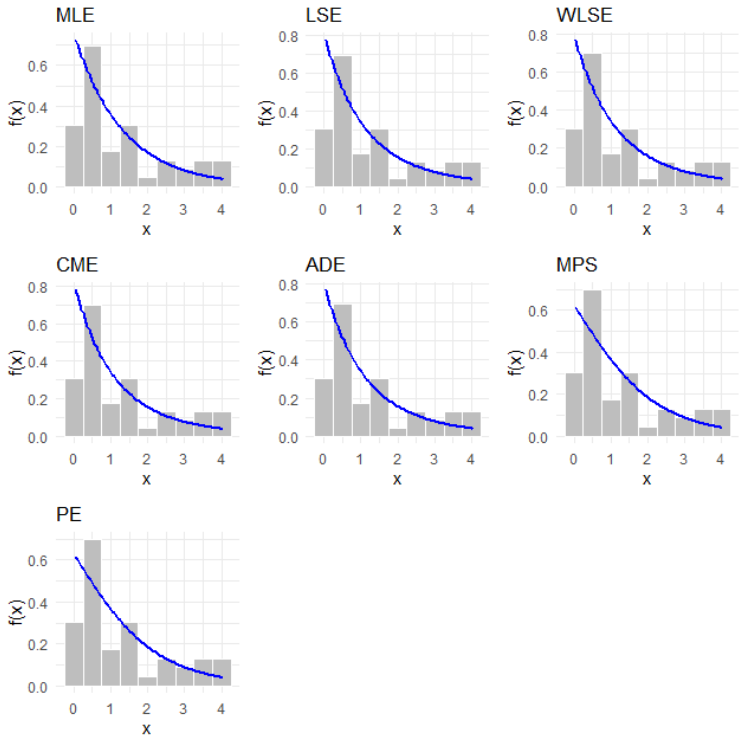


Figure 12. Graphical comparison of estimated PDF for dataset II.

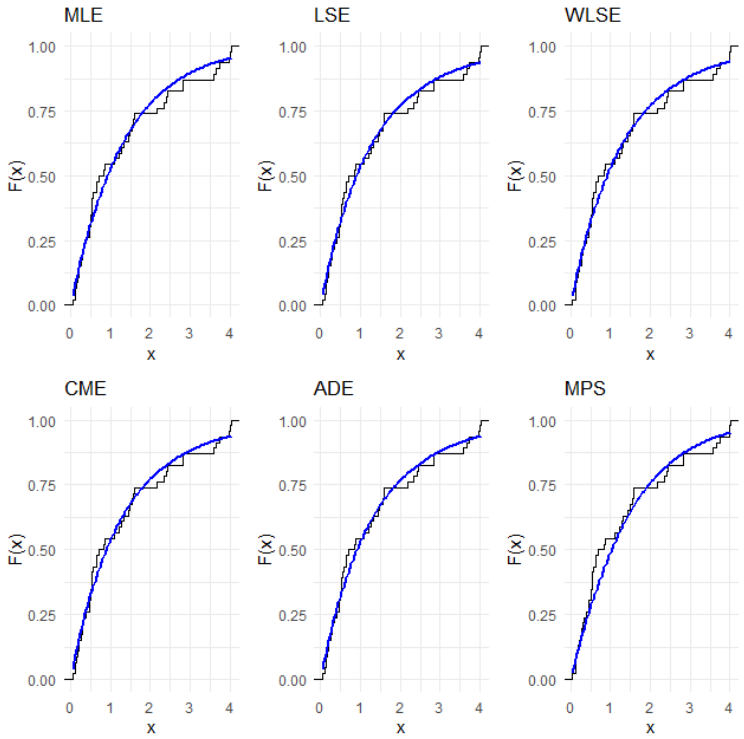


Figure 13. Graphical comparison of estimated CDF for dataset II.

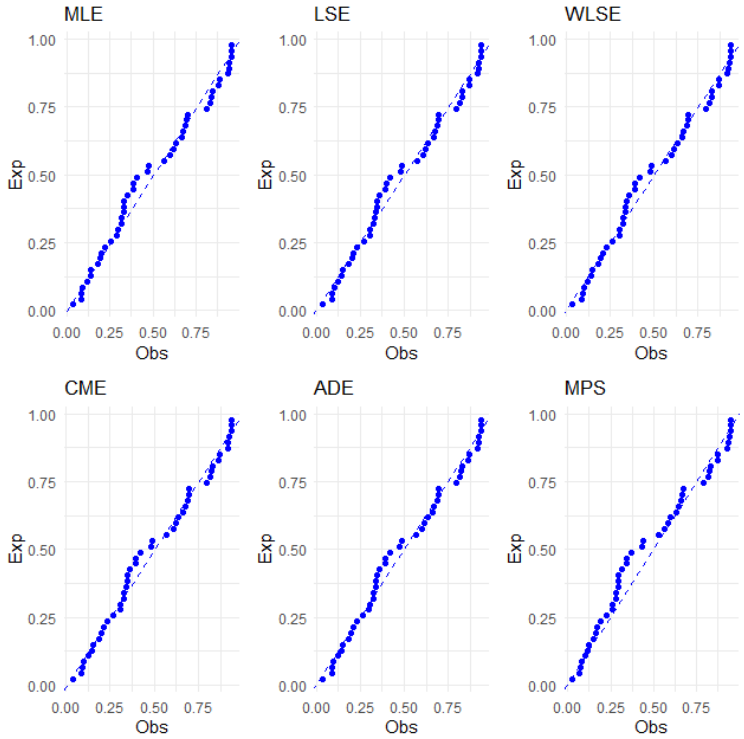


Figure 14. Graphical comparison of P-P plots for dataset II.

for Dataset I and 0.9032 for Dataset II), confirming that the TP distribution offers highly reliable inference under practical, noisy data conditions.
- The empirical results show that the TP model captures the key features of the two datasets more effectively than the competing models. Both datasets are right-skewed with heavy tails, and the TP model attains the lowest AIC, BIC, CAIC, HQIC and K-S values with the highest p-values. The TP model also accommodates non-monotonic hazard rates, which is important for the biomedical survival data where mortality risk peaks early and then stabilize. These features matter in practice: improved tail and skewness modeling enhances failure-probability estimation and maintenance scheduling in reliability engineering, while flexible hazard modeling improves early-mortality risk and long-term survival estimation in biomedical practice.

8. Conclusion

This research presented the transmuted Perk (TP) distribution, a versatile three-parameter model designed to address the complexities of skewed and variable lifetime data. We derived explicit mathematical properties, including moments, quantile function, order statistics, probability weighted moments, and Rényi entropy. Through an extensive simulation study evaluating seven estimation approaches, we demonstrated the stability and finite-sample efficiency of the model parameters, with the Maximum Product of Spacings (MPSE) and Cramér–von Mises (CME) methods showing high precision. Empirical validation across engineering failure intervals and oncology survival times confirmed that the TP model provides a superior fit compared to baseline and related Perk extensions, as evidenced by lower information criteria and higher goodness-of-fit p-values.

The TP distribution offers clear practical advantages for real-world risk and reliability analysis. In reliability engineering, its capacity to model non-monotonic and increasing failure rates allows engineers to more accurately assess component degradation trends and optimize preventive maintenance schedules, preventing premature failures in critical machinery. In biomedical applications, particularly clinical oncology, the model's flexible hazard structure effectively captures the acute early post-treatment mortality risk alongside long-term patient survival, facilitating better prognostic evaluation.

Directions for Future Research. Building upon the foundational results established in this work, several promising research avenues emerge:

- Censored Data Frameworks: Extending the TP model inference to accommodate Type-I, Type-II, and progressive censoring schemes, which are standard in industrial stress testing and clinical trials.
- Advanced Bayesian Methodologies: Investigating Bayesian estimation using informative conjugate/non-conjugate priors under asymmetric loss functions (LINEX and General Entropy loss) to further improve parameter estimation accuracy in small-sample contexts.
- Regression and Bivariate Extensions: Developing a transmuted Perk regression model for covariate analysis, as well as constructing bivariate and multivariate extensions to model correlated lifetime components in complex systems.

Acknowledgment

The authors extend their appreciation to Umm Al-Qura University, Saudi Arabia for funding this research work through grant number: 26UQU4340323GSSR04.

Funding Statement

This research work was funded by Umm Al-Qura University, Saudi Arabia under grant number: 26UQU4340323GSSR04.

REFERENCES

1. E. J. Green, F. A. Roesch Jr, A. F. Smith, and W. E. Strawderman, *Bayesian estimation for the three-parameter Weibull distribution with tree diameter data*, Biometrics, pp. 254–269, 1994.
2. A. R. El-Alosey, M. Elgarhy, and A. M. Gemeay, *A new unit generated family of distributions: Classical estimation methods and applications to real data*, Statistics, Optimization & Information Computing, vol. 16, no. 5, pp. 4202–4243, 2026.
3. M. Elgarhy, N. F. Hekal, M. M. El Genidy, A. R. Mohamed, and K. M. A. Mahfouz, *A new generalization of double XRamma distribution: Statistical properties and applications to real data*, Statistics, Optimization & Information Computing, vol. 16, no. 5, pp. 5220–5246, 2026.
4. F. Jamal, M. Arslan Nasir, G. Ozel, M. Elgarhy, and N. Mamode Khan, *Generalized inverted Kumaraswamy generated family of distributions: theory and applications*, Journal of Applied Statistics, vol. 46, no. 16, pp. 2927–2944, 2019.
5. S. A. Alyami, M. G. Babu, I. Elbatal, N. Alotaibi, and M. Elgarhy, *Type II half-logistic odd Fréchet class of distributions: Statistical theory and applications*, Symmetry, vol. 14, no. 6, 1222, 2022.
6. A. Z. Afify, G. M. Cordeiro, N. A. Ibrahim, F. Jamal, M. Elgarhy, and M. A. Nasir, *The Marshall-Olkin odd Burr III-G family: theory, estimation, and engineering applications*, IEEE Access, vol. 9, pp. 4376–4387, 2020.
7. H. M. Yousof, A. Z. Afify, M. Alizadeh, N. S. Butt, G. G. Hamedani, and M. M. Ali, *The transmuted exponentiated generalized-G family of distributions*, Pakistan Journal of Statistics and Operation Research, pp. 441–464, 2015.
8. A. Algarni, A. M. Almarashi, I. Elbatal, A. S. Hassan, E. M. Almetwally, A. M. Daghistani, and M. Elgarhy, *Type I half logistic Burr X-G family: properties, Bayesian, and non-Bayesian estimation under censored samples and applications to COVID-19 data*, Mathematical Problems in Engineering, vol. 2021, no. 1, 5461130, 2021.
9. J. T. Eghwerido, L. C. Nzei, A. E. Omotoye, and F. I. Agu, *The Teissier-G family of distributions: Properties and applications*, Mathematica Slovaca, vol. 72, no. 5, pp. 1301–1318, 2022.
10. Y. Y. Abdelall, A. S. Hassan, and E. M. Almetwally, *A new extention of the odd inverse Weibull-G family of distributions: Bayesian and non-Bayesian estimation with engineering applications*, Computational Journal of Mathematical and Statistical Sciences, vol. 3, no. 2, pp. 359–388, 2024.
11. M. N. Atchadé, A. A. Agbahide, T. Otodji, M. J. Bogninou, and A. Moussa Djibril, *A new shifted Lomax-X family of distributions: Properties and applications to actuarial and financial data*, Computational Journal of Mathematical and Statistical Sciences, vol. 4, no. 1, pp. 41–71, 2025.
12. W. T. Shaw, and I. R. Buckley, *The alchemy of probability distributions: Beyond Gram-Charlier & Cornish-Fisher expansions, and skew-normal or kurtotic-normal distributions*, Submitted, Feb, 7, 64, 2007.
13. B. Saraçoğlu, and C. Tanış, *A new lifetime distribution: transmuted exponential power distribution*, Communications Faculty of Sciences University of Ankara Series A1 Mathematics and Statistics, vol. 70, no. 1, pp. 1–14, 2021.
14. M. M. Gharaibeh, and A. I. Al-Omari, *Transmuted Ishita distribution and its applications*, Journal of Statistics Applications & Probability, vol. 8, no. 2, pp. 67–81, 2019.
15. L. Al-Zou'bi, *Transmuted Mukherjee-Islam distribution: a generalization of Mukherjee-Islam distribution*, Journal of Mathematics Research, vol. 9, no. 4, pp. 135–144, 2017.
16. A. I. Al-Omari, A. M. Al-khazaleh, and L. M. Alzoubi, *Transmuted Janardan distribution: A generalization of the Janardan distribution*, Journal of Statistics Applications and Probability, vol. 5, no. 2, pp. 1–11, 2017.
17. M. Elgarhy, D. S. Metwally, A. S. Hassan, and A. W. Shawki, *A new generalization of power Chris–Jerry distribution with different estimation methods, simulation and applications*, Scientific African, e02769, 2025.
18. N. M. Eze, and W. B. Yahya, *Transmuted exponential-compound Weibull distribution for modelling of positively skewed data*, Scientific African, e02725, 2025.
19. E. A. Eldessouky, O. H. M. Hassan, B. Aloraini, and I. Elbatal, *Modeling to medical and economic data using: The transmuted power unit inverse Lindley distribution*, Alexandria Engineering Journal, vol. 113, pp. 633–647, 2025.
20. M. M. Abdelwahab, D. A. Ramadan, S. Kumar, M. M. Hasaballah, and A. M. El Gazar, *Statistical analysis of the induced Ailamujia lifetime distribution with engineering and biomedical applications*, Mathematics, vol. 13, no. 20, 3307, 2025.
21. A. M. El Gazar, M. M. Abdelwahab, M. M. Hasaballah, and D. A. Ramadan, *Applied statistical modeling using the truncated Perk distribution: Estimation methods and multidisciplinary real-data applications*, Axioms, vol. 14, no. 8, 627, 2025.
22. W. Perks, *On some experiments in the graduation of mortality statistics*, Journal of the Institute of Actuaries, vol. 63, no. 1, pp. 12–57, 1932.
23. S. J. Richards, *Applying survival models to pensioner mortality data*, British Actuarial Journal, vol. 14, no. 2, pp. 257–303, 2008.
24. B. Singh, and N. Choudhary, *The exponentiated Perks distribution*, International Journal of System Assurance Engineering and Management, vol. 8, pp. 468–478, 2017.
25. I. Elbatal, N. Alotaibi, E. M. Almetwally, S. A. Alyami, and M. Elgarhy, *On odd Perks-G class of distributions: properties, regression model, discretization, Bayesian and non-Bayesian estimation, and applications*, Symmetry, vol. 14, no. 5, 883, 2022.
26. N. Hussain, M. H. Tahir, F. Jamal, S. Shafiq, N. Alsadat, M. Elgarhy, ..., and V. B. Nagarjuna, *Comparison of different estimation methods for the inverse power Perk distribution with applications in engineering and actuarial sciences*, Physica Scripta, vol. 99, no. 10, 105232, 2024.
27. J. A. Greenwood, J. M. Landwehr, N. C. Matalas, and J. R. Wallis, *Probability weighted moments: definition and relation to parameters of several distributions expressable in inverse form*, Water Resources Research, vol. 15, no. 5, pp. 1049–1054, 1979.
28. A. Rényi, *On measures of entropy and information*, in Proceedings of the Fourth Berkeley Symposium on Mathematical Statistics and Probability, Volume 1: Contributions to the Theory of Statistics, vol. 4, pp. 547–562, University of California Press, 1961.
29. C. Tsallis, *Possible generalization of Boltzmann-Gibbs statistics*, Journal of Statistical Physics, vol. 52, pp. 479–487, 1988.
30. G. Alomani, M. Kayid, and A. M. Elgazar, *Statistical analysis of radiation data using power unit moment exponential distribution*, Journal of Radiation Research and Applied Sciences, vol. 18, no. 2, 101432, 2025.
31. J. J. Swain, S. Venkatraman, and J. R. Wilson, *Least squares estimation of distribution functions in Johnson's translation system*, Journal of Statistical Computation and Simulation, vol. 29, no. 4, pp. 271–297, 1988.

32. K. Choi, and W. G. Bulgren, *An estimation procedure for mixtures of distributions*, Journal of the Royal Statistical Society Series B: Statistical Methodology, vol. 30, no. 3, pp. 444–460, 1968.
33. T. W. Anderson, and D. A. Darling, *Asymptotic theory of certain goodness-of-fit criteria based on stochastic process*, Annals of Mathematical Statistics, vol. 23, pp. 193–212, 1952.
34. S. J. Press, *Subjective and objective Bayesian statistics: principles, models, and applications*, John Wiley & Sons, 2009.
35. A. M. El Gazar, D. A. Ramadan, M. ElGarhy, and B. S. El-Desouky, *Estimation of parameters for inverse power Ailamujia and truncated inverse power Ailamujia distributions based on progressive type-II censoring scheme*, Innovation in Statistics and Probability, vol. 1, no. 1, pp. 76–87, 2025.
36. A. M. Abouammoh, and A. M. Alshingiti, *Reliability estimation of generalized inverted exponential distribution*, Journal of Statistical Computation and Simulation, vol. 79, no. 11, pp. 1301–1315, 2009.
37. P. E. Oguntunde, and A. O. Adejumo, *The transmuted inverse exponential distribution*, International Journal of Advanced Statistics and Probability, vol. 3, no. 1, pp. 1–7, 2015.
38. D. N. P. Murthy, M. Xie, and R. Jiang, *Weibull Models*, John Wiley & Sons, New York, 2004.
39. A. Tahani et al., *Estimation of the unknown parameters for the compound Rayleigh distribution based on progressive first-failure-censored sampling*, Open Journal of Statistics, vol. 1, pp. 161–171, 2011.
40. S. O. Bashiru, M. Kayid, R. M. Sayed, O. S. Balogun, A. T. Hammad, and M. M. Abd El-Raouf, *Transmuted inverse unit Teissier distribution: Properties, estimations and applications to medical and radiation sciences*, Journal of Radiation Research and Applied Sciences, vol. 18, no. 1, 101208, 2025.
41. S. O. Bashiru, A. M. Isa, A. A. Khalaf, M. A. Khaleel, K. C. Arum, and C. L. Anioke, *A hybrid cosine inverse Lomax-G family of distributions with applications in medical and engineering data*, Nigerian Journal of Technological Development, vol. 22, no. 1, pp. 261–278, 2025.
42. Z. Shah, Z. Ahmad, Z. Almaspoor, F. Khan, C. K. Onyekwere, and G. Rao, *A new logarithmic pie power-G family of distributions: Properties and applications to medical and traffic data*, Modern Journal of Statistics, vol. 2, no. 2, pp. 129–158, 2026.
43. A. Djebar, O. A. Alqasem, H. Zeghdoudi, S. O. Bashiru, and A. M. Gemeay, *A polynomial family based on reliability function: Properties, estimation methods, and applications*, Reliability Engineering & System Safety, 113145, 2026.
44. A. A. H. Ahmadini, B. Elkalzah, K. Elsharkawy, and G. A. Marei, *Reliability estimation of s-out-of-k systems under inverted Z-Lindley stress-strength models with progressive censoring: an engineering application*, Quality and Reliability Engineering International, 2026, https://doi.org/10.1002/qre.70391.
45. A. A. H. Ahmadini, M. Elwahab, M. Elgarhy, H. Aljohani, and G. A. Marei, *Modulating early-life risk without breaking Weibull structure: an odds-based Weibull model for engineering failure-time data*, Revista Internacional de Métodos Numéricos para Cálculo y Diseño en Ingeniería, vol. 42, no. 6, 2026, https://doi.org/10.23967/j.rimni.2026.10.82546.
46. A. H. Alenezy, L. S. Diab, K. A. Rashedi, and G. A. Marei, *Inference for a step-stress model under the inverted Z-Lindley distribution with progressive Type-II censoring*, AIMS Mathematics, vol. 11, pp. 31919–31962, 2026.
47. A. H. Alenezy, B. Elkalzah, A. F. I. Alahshan, and G. A. Marei, *Robust inference for stress-strength reliability of the Garhy distribution under diverse record schemes with engineering and medical applications*, Mathematics, vol. 14, 1940, 2026.
48. A. H. Alenezy, K. A. Rashedi, A. B. Ghorbal, and G. A. Marei, *Bridging Markov chain Monte Carlo techniques and Tierney–Kadane approximations for progressively censored Garhy reliability models: simulation insights and a medical application*, Mathematics, vol. 14, 1777, 2026.
49. B. Elkalzah, M. O. Mohamed, K. Elsharkawy, E. S. Osman, A. Aldukeel, and G. A. Marei, *Classical and Bayesian estimation of stress-strength reliability under the discrete alpha-power Weibull distribution with incomplete and record data: application to high-voltage capacitors*, AIMS Mathematics, vol. 11, pp. 6374–6399, 2026.
50. M. Imran, M. A. F. Elbarkawy, F. Jamal, and G. A. Marei, *An extended Lindley model with applications to entropy-based loss and actuarial risk measures*, Computational Journal of Mathematical and Statistical Sciences, vol. 5, pp. 1–33, 2026.
51. S. Benchiha, L. P. Sapkota, A. Al Mutairi, V. Kumar, R. H. Khashab, A. M. Gemeay, et al., and S. G. Nassr, *A new sine family of generalized distributions: Statistical inference with applications*, Mathematical and Computational Applications, vol. 28, no. 4, p. 83, 2023.
52. M. N. Atchadé, M. A. N'bouké, A. M. Djibril, A. Al Mutairi, M. S. Mustafa, E. Hussam, et al., and S. G. Nassr, *A new Topp-Leone Kumaraswamy Marshall-Olkin generated family of distributions with applications*, Heliyon, vol. 10, no. 2, 2024.
53. A. S. Al-Moisheer, I. Elbatal, W. Almutiry, and M. Elgarhy, *Odd inverse power generalized Weibull generated family of distributions: Properties and applications*, Mathematical Problems in Engineering, vol. 2021, no. 1, p. 5082192, 2021.
54. S. M. Alghamdi, M. Shrahili, A. S. Hassan, R. E. Mohamed, I. Elbatal, and M. Elgarhy, *Analysis of milk production and failure data: using unit exponentiated half logistic power series class of distributions*, Symmetry, vol. 15, no. 3, p. 714, 2023.
55. N. Alsadat, M. Imran, M. H. Tahir, F. Jamal, H. Ahmad, and M. Elgarhy, *Compounded Bell-G class of statistical models with applications to COVID-19 and actuarial data*, Open Physics, vol. 21, no. 1, p. 20220242, 2023.
56. G. A. Marei, D. Basalamah, S. G. Nassr, A. W. Shawki, and M. Elgarhy, *On the Marei distribution: a novel one-parameter model with applications*, Applied Mathematics & Information Sciences, vol. 20, pp. 1407–1426, 2026.
57. K. A. Rashedi, L. S. Diab, A. H. Alenezy, and G. A. Marei, *A one-parameter decreasing-hazard lifetime model with exact inference on a bounded-below support*, AIMS Mathematics, vol. 11, pp. 24445–24489, 2026.
58. K. A. Rashedi, L. S. Diab, A. H. Alenezy, and G. A. Marei, *Inference for stress-strength reliability under unified hybrid censoring: a one-parameter model with applications*, Mathematics, vol. 14, 2041, 2026.